Research Article

Global Atmospheric CO2 Lags Temperature by 150 yr between 1 and 1850 AD

Ronald Grabyan

Irvine, California, USA

Klimarealistene
Vollsveien 109
1358 Jar, Norway
ISSN: 2703-9072

Correspondence:
rgrabyan@cox.net

Vol. 5.3 (2025)
pp. 35-80

Abstract

This study investigates whether atmospheric CO_2 precedes or lags global temperature changes over the past 2000 yr, using both visual and statistical analyses. A parallel evaluation of Total Solar Irradiance (TSI) and temperature was conducted to assess the influence of solar forcing on climate variability.

Temperature, CO_2, and TSI data were drawn from many well-established publications and international climate data repositories. Original, unsmoothed series were used to identify visual markers—such as peak–trough alignments, correlative clusters, and trend concordance—while smoothed series (using 50-yr and 100-yr running averages and Loess filters) were employed to emphasize large-scale patterns and reduce local variability. Correlation analysis, conducted within a statistical validation framework, was applied across all data variants.

Results show that atmospheric CO_2 consistently lags temperature by approximately 150 yr from 1 to 1850 AD. After applying this lag correction (CO_{2Lag}), Pearson correlation coefficients (r_{PCC}) between CO_{2Lag} and temperature reached Very Strong values ranging from 0.85 to 0.99. TSI–temperature correlations were generally Strong across the full 2000 yr interval, and Very Strong from 1850 to present. A prominent alignment among CO_{2Lag}, TSI, and temperature occurs around 1460 AD.

These findings indicate that atmospheric CO_2 does not precede, nor appear to drive, global temperature trends. Rather, CO_2 consistently lags temperature, suggesting it functions as a response variable rather than a primary forcing. In addition, TSI exhibits Strong to Very Strong temporal alignment with temperature, supporting the hypothesis that solar variability plays a significant role in long-term climate change.

Keywords: CO_2; temperature; CO_2 lags temperature; total solar irradiance; last 2000 yr

Submitted 2024-12-17, Accepted 2025-08-20. https://doi.org/10.53234/scc202510/04

1. Introduction

Understanding the role of atmospheric CO_2 in climate dynamics is a critical scientific and policy concern. If CO_2 is a primary driver of global temperature change, then reducing anthropogenic emissions becomes essential. Conversely, if CO_2 plays a lagging role, the rationale for large-scale mitigation strategies deserves reexamination. A rigorous, evidence-based evaluation of this relationship is needed.

The prevailing consensus in climate science maintains that increased atmospheric CO_2—primarily from fossil fuel combustion—drives warming of the Earth's surface and lower atmosphere. This conclusion is supported by numerous studies linking rising CO_2 levels to temperature trends across multiple timescales. However, other peer-reviewed studies challenge this causality, suggesting that temperature changes lead CO_2 changes, rather than follow them (e.g., Humlum et

al., 2013; Chylek et al., 2018a; Sharma & Karamanev, 2021). Some of these studies show temperature leading CO_2 by centuries in paleoclimate records, while others find leads of months in the instrumental era and millions of years in the distant paleoclimate records.

Recent publications further support the hypothesis that temperature changes precede atmospheric CO_2 fluctuations. Several studies by Koutsoyiannis and collaborators (2020, 2022a, 2022b, 2023, 2024a, 2024b) suggest that global air temperature may act as leading indicators or drivers of CO_2 concentration changes.

In addition to the CO_2-temperature relationship, a wide array of natural factors has been proposed to explain historical temperature variability. These include:

1. Solar variability: Total Solar Irradiance (TSI), magnetic modulation of cosmic rays, UV-induced atmospheric chemistry, and weakening of the jet stream (Easterbrook, 2016a; Svensmark and collaborators, 1999, 2007, 2016, 2021, 2022; Ogurtson et al., 2002; Shaviv et al., 2023; Scafetta, 2023; Gray et al., 2010; Moffa-Sanchez et al., 2014; Ineson et al., 2011).
2. Oceanic oscillations: The Atlantic Multidecadal Oscillation (AMO), thermohaline circulation, and ENSO-like cycles (Knudsen et al., 2011; Lin & Qian, 2022; Gray, 2012; Gray et al., 2003; D'Aleo & Easterbrook, 2016; Doos et al., 2012; Toggweiler & Key, 2001).
3. Planetary and orbital forcing: Changes in Earth's eccentricity, axial tilt, and precession (Milankovitch cycles), as well as planetary gravitational influences (Scafetta & Bianchini, 2022; Stefani et al., 2004; Wanner et al., 2022; Morner, 2012; Lourens & Tuenter, 2016; Marsh, 2014; Roe, 2006; Shackleton, 2000; Imbrie et al., 1992).
4. Volcanism, tectonics, and extraterrestrial impacts: Volcanic aerosols, plate tectonics, and meteor strikes as agents of climate change (Covey et al., 1994; Dekan, 2021; Komitov & Kaftan, 2020; Wanner et al., 2022; Vinos, 2024a; Vinos, 2024b; Vevard & Veizer, 2019).

Multiple studies across diverse timescales have found that CO_2 tends to lag temperature. For instance:

1. Ice core records from the last 420 kyr show lags of 300 to 2300 yr (Mudelsee, 2001; Caillon et al., 2003).
2. Monnin et al. (2001) reported a lag of ~410,000 yr between 11.2 and 17 kyr BP.
3. Sharma and Karamanev (2021) found CO_2 lagging temperature by 1020–1080 yr over the last 650 kyr.
4. Middleton (2011) postulated a 250-yr lag of CO_2 to temperature during the Little Ice Age.
5. Instrumental records from 1980–2011 show CO_2 lagging SST and air temperatures by 9 to 12 mo (Humlum et al., 2013).
6. Monthly datasets for the 1960–2016 period show average lags of 4 to 5 mo (Adams & Piovesan, 2005; Chylek et al., 2018b).
7. Koutsoyiannis (2024a) synthesized findings across multiple geological intervals, reporting that CO_2 consistently lagged temperature, with lag duration increasing with timescale:
   7.1. Phanerozoic: ~2.3 million yr
   7.2. Cenozoic: ~800,000 yr
   7.3. Late Quaternary: ~1200 yr
   7.4. Common Era (1–1700 AD): ~33 yr
   7.5. Instrumental Period: 3–8 months

The consistent pattern of temperature leading CO_2 invites a reevaluation of cause-and-effect assumptions in climate science. This study focuses on the Common Era, analyzing the lag relationship between CO_2 and temperature using 16 global temperature proxies and 4 CO_2 proxies over the past 2000 yr. Both visual and statistical methods (e.g., statistically validated Pearson correlation, lag testing) are employed.

Results show that CO_2 consistently lags temperature by approximately 150 yr across the 1–1850 AD period. These findings hold for both the pre-1600 and post-1600 segments of the data, even accounting for structural breaks or regime shifts.

Given the robust pattern of temperature leading CO_2, this analysis is extended to evaluate potential drivers of temperature change. Numerous studies have pointed to solar variability as a plausible mechanism, including changes in TSI (Scafetta, 2023; D'Aleo, 2016; Whiteet al., 1997; White, 2000; Hoyt & Schatten, 1993; Soon, 2009; Soon & Legates, 2013; Soon et al., 2015, Li, 2022; Wang et al., 2020; Schmutz, 2021; Usoskin et al., 2005; Douglass & Clader, 2002; Abdussamatov, 2016; Lean, 2000), solar magnetic activity (Lockwood & Stamper, 1999), and radiative forcing beyond TSI alone (Shaviv, 2008). Though satellite measurements since 1978 show only ~0.1% variation in TSI over an 11 yr solar cycle (Willson & Hudson, 1988), longer-term changes since the Maunder Minimum may be as high as 0.4–0.5% (Willson, 1997; Hoyt & Schatten, 1997; Solanki & Fligge, 2000; Willson & Mordvinov, 2003).

In addition to variations in TSI, several studies have proposed more indirect solar influences on climate. These include solar eruptions such as flares, coronal mass ejections, and high-speed wind streams from coronal holes (D'Aleo, 2016). Since 2001, the total magnetic flux emitted by the Sun has reportedly increased by a factor of 2.3, which may influence Earth's climate through two primary mechanisms: (1) enhanced ozone chemistry in the upper atmosphere triggered by ultraviolet radiation (Bard & Frank, 2006; Gray et al., 2010; Haigh et al., 2010; Ermolli et al., 2013), and (2) ionization at higher latitudes during geomagnetic storms (D'Aleo, 2016; Lockwood & Stamper, 1999). In parallel, variations in cloud formation linked to galactic cosmic rays and solar modulation have been suggested as additional contributors to climate variability (Svensmark & Friis-Christensen, 1997; Svensmark, 1999, 2007, 2016, 2022; Svensmark et al., 2021; Shaviv et al., 2023).

Abdussamatov (2015) further argued that Earth's temperature is influenced by the annual energy balance, incorporating factors such as TSI, oceanic thermal inertia, albedo feedback, and greenhouse gas concentrations. According to D'Aleo (2016), these indirect solar effects may significantly amplify the Sun's role in modulating climate.

This study evaluates solar irradiance records from multiple sources and compares them to global temperature over the last two millennia and selected modern periods (1659, 1850, 1880 to present). While causation cannot be definitively established, the correlations observed suggest that solar energy input—direct and indirect—plays a substantial role in global temperature variability.

Four Appendices for this study are incorporated in the Supplementary Material, including Appendices A–D: (A) Data – Correlation Analysis of CO_2 vs. temperature, (B) Statistical Validation Framework, (C) Structural Break or Regime Shift at 1600 AD, and (D) Total Solar Irradiance and Temperature.

2. Methods

Published data from 18 studies of air temperature and five studies of CO_2 across the last 2000 yr were used in this investigation. Multiple proxies from across the world were utilized in these published studies of CO_2 and temperature. For CO_2, ice cores from Antarctica were used in this study. For temperature, ice cores, tree rings, marine and lake sediment, speleothem, pollen, Mg/Ca in fossil shells, and stalagmites, and others, were also used in these studies.

Data from the published studies were either obtained from the respective authors, downloaded from public repositories or digitized from the published papers utilizing an online digitizing program, Graph Grabber v2.0.2 (Quintessa Limited, 2020) – all with permission. Each temperature study was compared to each CO_2 study (64 pairs in the main body of this report – Data Set A and Data Set B).

Results of r_{PCC} data analysis for Data Set A and Data Set B, for data ranges of 200-1600 AD and 1000-1600 AD are presented in Supplementary Material, Appendix A.

The research plan of this paper includes using Pearson Correlation Coefficients obtained by evaluating each pair of CO_2 and temperature time-series data obtained from various published studies, both in original form, data smoothing transformations, and with CO_2 at a range of lags from -200 to +200 yr in an interval of 10 yr. Therefore, it is important to discuss the potential weaknesses of this approach as presented by Koskinas et al. (2022) and Koutsoyiannis (2024c), as well as the potential strengths. These studies address the strong time-dependence of such data, especially of long-range memory type (Hurst-Kolmogorov dynamics) where the probability distribution of r_{PCC} is potentially heavily modified by the presence of long-range dependence (LRD). Long memory processes imply persistent autocorrelation that can inflate apparent statistical significance of cross-correlations and cause unreliable p-values.

The well-described concerns regarding long-range dependence (LRD) in paleoclimate CO_2 and temperature data — as outlined by Koskinas et al. (2022) and Koutsoyiannis (2024c) — are fully acknowledged, and these concerns center on the potential inflation of correlation coefficients when applied to nonstationary or persistent time series. However, based on a structured series of diagnostic tests and methodological guard rails (herein termed Statistical Validation Framework, as described below), I consider the conditional use of Pearson Correlation Coefficient (r_{PCC}) both acceptable and informative within the context of this study and pending the results of the SVF (Beran, 1994; Granger & Joyeux, 1980). The following measures support this judgment:

1. Alignment of time-series by calendar-year, with a consistent shift 150 yr earlier in time applied to CO_2, testing the hypothesized delayed or lagged response to temperature
2. Multiple smoothing levels (Original, RA 100, multiple Loess) applied to isolate persistent structure while at the same time observing inflation risk
3. Visual inspection of CO_2 and temperature curve alignment which in most cases depicts strong shape and change similarity consistent with lagged response, including alignment of peaks and troughs
4. Max-r-lag testing across a broad range of lag intervals (-200 to +200 yr) to identify the peak r-correlations with physical lags (generally at an interval of 10 yr)
5. Statistical Validation Framework:

    5.1 Autocorrelation Tests:
        5.1.1 Durbin-Waston Test (Durbin & Watson, 1950)
        5.1.2 Breusch-Godfrey Test (Breusch, 1978; Godfrey, 1978)
        5.1.3 Ljung-Box Q-Test (Ljung & Box, 1978)

    5.2 Hurst Exponent Analysis:
        5.2.1 Rescaled Range (R/S) (Hurst, 1951)
        5.2.2 Detrended Fluctuation Analysis (DFA) (Peng et al., 1994)
        5.2.3 Geweke-Porter-Hudak Spectral Estimation (GPH) (Geweke & Porter-Hudak, 1983)

    5.3 Heteroskedasticity and Autocorrelation Consistent Standard Errors (HAC SE) (Newey & West, 1987)

    5.4 Effective Sample Size (Neff) (Newey & West, 1987; Bretherton et al., 1999)

    5.5 Block Permutation Results (Politis & Romano, 1994)

    5.6 False Discovery Rate Methods (Globally Grouped) (Benjamini & Hochberg, 1995)

    A complete discussion of these tests with their results can be found in Supplementary Material, Appendix B, in the context of the Statistical Validation Framework (SVF) -- validation of correlation significance under dependence, autocorrelation, and long-memory

conditions.

Total Solar Irradiance (TSI) data were analyzed and compared to the temperature data utilized in this study in order to observe potential correlations. 11 TSI studies were included, and six temperature studies from 1659, 1850 and 1880 were included to address the near-term timeframe of 200 to 400 yr as well as the last 2000 yr timeframe.

Visual graphical analysis, in conjunction with various smoothing algorithms, assisted in the qualitative and semi-quantitative search for understanding the relationship in our climate of:

CO_2 and temperature
TSI and temperature

The methods process of this study is identified and followed as shown in detail below:

1. Each data set (from published sources) was evaluated in its original state and processed with a straight-line interpolation algorithm resulting in a data set of whole number years with an interval of one, unless it was already presented as such.
2. Each resulting data set was graphed as comparison graphs of every CO_2-temperature pair. Vertical axes adjustments were made to overlay the graphs to similar curve amplitudes in order to visually compare the curves.
3. The average lag of CO_2 to temperature was determined to be about 150 yr, based on a max-lag analysis with a range of -200 to +200 yr – the CO_{2Lag} curves were added to the charts with original non-smoothed CO_2 and non-smoothed temperature.
4. In order to remove noise and other more granular data influences, and reveal larger trends, each data set was smoothed in Excel Professional 2019, using 4 algorithms:

   4.1. Running Average, centered on 50 yr (RA 50)
   4.2. Running Average, centered on 100 yr (RA 100)
   4.3. Loess Smoothing Algorithm – less smoothing (Loess 1)
   4.4. Loess Smoothing Algorithm – more smoothing (Loess 2)

   Loess (Locally Estimated Scatterplot Smoothing) is an Excel plugin, non-parametric locally weighted smoothing algorithm, with a smoothing parameter and the number of years for the quadratic moving regression (Peltier Tech, 2024).
5. Several iterations of selecting the appropriate Loess smoothing parameters were constructed in order to have resulting curves which had similar amplitude and frequency. If these two elements of the curves are not compatible, they may not reflect the true relationship of the curves, and statistical correlation could be poor and misleading. Note a larger number of data points (yr) in the Loess smoothing parameter will remove noise and other local features providing a broader, more regional view of the data. When smoothing data, the smoothed result is reflecting the impact of up to several hundred yr surrounding each data point (yr), and the localized nature of the original data will influence the smoothed curves. Thus, detailed temporal analysis with smoothed curves should be conducted with caution.
6. Pearson Correlation Coefficient (r_{PCC}) was calculated conditionally for each data pair of CO_2 and temperature, where there were data values at each year of both curves (64 sets for Data Set A and Data Set B)—data ranges 200-1600 AD, 1000-1600 AD, and 1600-1850 AD. An in-depth lag analysis approach was implemented where an r_{PCC} was calculated for each lag between -200 yr and +200 yr, and the maximum r_{PCC} was selected with its corresponding lag, along with an r_{PCC} at 0-lag, as well as r_{PCC}. These calculations resulted in tables and graphs of r_{PCC} as a function of lag correction, thus identifying the CO_2 lag year with the highest correlation. All r_{PCC} values are considered conditional as previously

mentioned. For this study the following correlation coefficient strength ranges are utilized for general strength of correlation:

$r_{PCC} > 0.00$ and $r_{PCC} < 0.20$	None
$r_{PCC} > 0.20$ and $r_{PCC} < 0.40$	Weak
$r_{PCC} > 0.40$ and $r_{PCC} < 0.60$	Moderate
$r_{PCC} > 0.60$ and $r_{PCC} < 0.80$	Strong
$r_{PCC} > 0.80$ and $r_{PCC} < 1.00$	Very Strong

7. Based on the general outline of the Statistical Validation Framework (SVF) described above, the detailed methodology and results are presented in Supplementary Material, Appendix B.
8. All statistical analyses were conducted using R (R Core Team, 2024) and Python 3.10 (Python Software Foundation). Analyses utilized the following libraries: numpy, scipy, pandas, and matplotlib in Python, and zoo, car, and nlme in R (Harris et al., 2020; Hunter, 2007; McKinney, 2010; Virtanen et al., 2020; Wickham, 2016; Zeileis & Grothendieck, 2005; Zeileis & Hothorn, 2002). Data alignment and preliminary Pearson correlation analyses were also implemented in Microsoft Excel using custom Visual Basic for Applications (VBA) scripts, which matched paired CO_2 and temperature values by calendar year (Microsoft Corporation, 2022). These routines served as independent verification of the primary results computed in R and Python. All figures in this study were created using Microsoft Excel's charting tools.
9. The data was separated into three main categories: (1) range 200-1600 AD, (2) range 1000-1600, and (3) range 1600-1850 AD. This is due to the presence of a structural break, possibly the result of a regime-shift at 1600 AD. This is discussed in Section 3.2 and in Supplementary Material, Appendix C. The data in the range 1600-1850 AD was treated more rigorously due to the character of CO_2 post-1600 AD. The following data transformation steps applied to both CO_2 and temperature for this range, except where noted, are followed:
    9.1. 50-yr centered running average – applied to suppress short-term fluctuation and emphasize low-frequency variability (Jones & Mann, 2004).
    9.2. Cubic Transformation – utilized to amplify long-term fluctuations and nonlinearly enhance larger variations in the CO_2 time series. This emphasizes major deviations while preserving the sign of the data, a paleoclimate technique used to highlight signal dynamics (Moberg et al., 2005).
    9.3. Standard Linear Detrending – fits a straight line to the data using least squares regression which isolates the stationary fluctuation component at the same time eliminating monotonic drift (Mann, 2004; Mudelsee, 2010)
    9.4. Normalization (min-max, 0-1) – Each series was subsequently normalized to the (0,1) interval using min-max scaling. This process allows for direct visual and statistical comparison of series with different magnitudes while preserving the relative shape of each curve (Wilkes, 2011).

    This data was then processed for r_{PCC} and lag values prior to tabulating and charting the results. Results are tabulated in Supplementary Material, Appendix A, Table A23.
10. Graphs of the original curves were produced showing the original curves and lagged original curves. Graphs of the smoothed curves were produced showing smoothed CO_2, smoothed temperature, and smoothed lagged CO_2 by the amount identified by the strongest correlation analysis and related lag, which usually corresponded to the visual correlation. Smoothing included Running Average (RA 50 and RA 100) and a matrix of Loess (level 1 and level 2). Documented on each graph is the recording of conditional r_{PCC} (max at lag) and r_{PCC} at 0-lag, as well as significance qualification from the SVF.

11. For the data range 200-1600 AD, a composite graph was produced with the top 8 smoothed temperature curves; all 4 of the ice-core-based lag-corrected CO_2 curves; an average curve of the temperature curves; and an average of the CO_{2Lag} curves.
12. Pearson Correlation Coefficient (r_{PCC}) was calculated conditionally between the two average curves of temperature and lag-corrected CO_2 (at the peak of CO_{2lag} correction).
13. TSI data and temperature data were utilized in this study in order to observe potential correlations and possible causation (correlation does not automatically equate to causation) (Supplementary Material, Appendix D). Visual graphics and statistical correlation techniques were applied to this data as described previously.

3. Results

3.1 Data Results - CO_2 vs. Temperature (200-1600 AD and 1000-1600 AD)

Pearson Correlation Analysis, r_{PCC}, and lag analysis were conducted on all pairs of CO_2 and temperature data analyzed in this study – both Data Set A and Data Set B (Supplementary Material, Appendix A). This included calculating r_{PCC} for all combinations of four published CO_2 data sets and 16 published temperature data sets (eight in each set) covering varying ranges between two major data ranges (200- 1600 AD, and 1000-1600 AD) for five smoothing transformation algorithms:

1. Original data (Orig)
2. Running Average – 50 (RA 50)
3. Running Average – 100 (RA 100)
4. Loess Smoothing 1 (Loess 1) less smoothed
5. Loess Smoothing 2 (Loess 2) more smoothed

This approach calculated the following for each transformation level of the data:

1. r_{PCC} (no lag of CO_2 to temperature)
2. r_{PCC} (maximum r_{PCC}) (calculated from -200 to +200 lag yr in 10-yr intervals)
3. lag (lag interval at the maximum r_{PCC})
4. Averages of each calculated parameter per CO_2 and temperature source

In Supplementary Material, Appendix A, Fig. A1 shows the lag value at the maximum r_{PCC} depicted for a pair of CO_2 and temperature series – Rubino et al. (2019) and Yang et al. (2002). Typical of almost every pair of CO_2 and temperature lag analysis curve analyzed in this study, the curve resembles a normal or slightly log-normal curve where the correlation-lag values climb rather smoothly from 0, or negative, r_{PCC} to a peak of maximum r_{PCC} at a lag in the general average range of +150 yr. The curve then declines at a similar pace to the incline to 0, or negative r_{PCC}. This pattern is extremely consistent. While the average is about a 150 yr CO_2 lag, various data combinations at different smoothing transformations range from about 100 to about 200 CO_2 lag to temperature.

The following tables in Supplementary Material, Appendix A, contain the results organized as follows:

Data Set A Table	Data Set B Table	Transformation	Range
Table A1	Table A12	Original	200-1600 AD
Table A2	Table A13	Original	1000-1600 AD
Table A3	Table A14	RA 50	200-1600 AD
Table A4	Table A15	RA 50	1000-1600 AD
Table A5	Table A16	RA 100	200-1600 AD
Table A6	Table A17	RA 100	1000-1600 AD
Table A7	Table A18	Loess 1	200-1600 AD

Table A8	Table A19	Loess 1	1000-1600 AD
Table A9	Table A20	Loess 2	200-1600 AD
Table A10	Table A21	Loess 2	1000-1600 AD

Tables A11 (Data Set A) and A22 (Data Set B) (as shown in Supplementary Material, Appendix A) identify the smoothing transformation parameters utilized, specifically the parameters for the Loess method. A general overview of the data in Tables A1 through A11 (as shown in Supplementary Material, Appendix A) are summarized in Table 1. The separation of results into the ranges (200-1600 AD and 1000-1600 AD) are predicated on a couple of factors:

1. Two of the four CO_2 data sets have data from well-before 1000 AD and the other two commence at around 1000 AD. Likewise, 10 of the 16 temperature data sets begin well before 1000 AD, and the other six commence around 1000 AD.
2. It appears there was a more sparsely sampled original sampling rate by the published authors pre-1000 AD than post-1000 AD, creating some uncertainty with the earlier data.
3. The calculated r_{PCC} data from the range of 200-1600 AD was consistently lower by about 0.20 than the data from the range of 1000-1600 AD.

A general overview of the data in Tables A12 through A22 (as shown in Supplementary Material, Appendix A) are summarized in Table 2.

Table 1. Summarizes the conditional r_{PCC} and lag data for Data Set A and five transformational levels (Original, RA 50, RA 100, Loess 1, and Loess 2) for two data ranges (200-1600 AD and 1000-1600 AD). This summary is based on the results shown in tables A1-A11 in Supplementary Material, Appendix A.

Summary of r_{PCC} Analysis Data Set A No Lag r_{PCC} and Maximum r_{PCC} with Corresponding Lag Five Transformation Levels and two Data Ranges (200-1600 AD, 1000-1600 AD)						
	Average r_{PCC}(no lag)	Average r_{PCC}(max lag)	Average lag	Range r_{PCC}(no lag)	Range r_{PCC} (max lag)	Range lag
Original						
200-1600 AD	-0.05	0.52	151	-0.38 to 0.16	0.47 to 0.57	90 to 180
1000-1600 AD	0.17	0.76	135	-0.13 to 0.38	0.60 to 0.92	60 to 160
RA 50						
200-1600 AD	0.02	0.66	152	-0.37 to 0.27	0.57 to 0.79	120 to 180
1000-1600 AD	0.30	0.87	132	0.07 to 0.60	0.77 to 0.96	60 to 170
RA 100						
200-1600 AD	0.04	0.71	153	-0.40 to 0.33	0.59 to 0.82	120 to 163
1000-1600 AD	0.45	0.91	128	0.08 to 0.81	0.81 to 0.95	80 to 160
Loess 1						
200-1600 AD	-0.01	0.61	151	-0.41 to 0.33	0.52 to 0.78	120 to 200
1000-1600 AD	0.25	0.85	132	-0.15 to 0.52	0.69 to 0.97	70 to 160
Loess 2						
200-1600 AD	0.02	0.68	155	-0.39 to 0.38	0.56 to 0.80	120 to 200
1000-1600 AD	0.35	0.92	127	-0.01 to 0.76	0.77 to 0.98	80 to 160
Averages						
200-1600 AD	0.00	0.64	152	-0.39 to 0.29	0.54 to 0.75	114 to 184
1000-1600 AD	0.30	0.86	131	-0.03 to 0.61	0.73 to 0.96	70 to 162

Table 2. Summarizes the conditional r_{PCC} and lag data for Data Set B and five transformational levels (Original, RA 50, RA 100, Loess 1, and Loess 2) for two data ranges (200-1600 AD and 1000-1600 AD). This summary is based on the results shown in tables A12-A22 in Supplementary Material, Appendix A.

Summary of r_{PCC} Analysis Data Set B No Lag r_{PCC} and Maximum r_{PCC} with Corresponding Lag Five Transformation Levels and two Data Ranges (200-1600 AD, 1000-1600 AD)						
	Average r_{PCC} (no lag)	Average r_{PCC} (max lag)	Average lag	Range r_{PCC} (no lag)	Range r_{PCC} (max lag)	Range lag
Original						
200-1600 AD	-0.24	0.41	154	-0.47 to -0.10	0.25 to 0.48	150 to 160
1000-1600 AD	0.08	0.59	128	-0.23 to 0.64	-0.10 to 0.87	100 to 200
RA 50						
200-1600 AD	-0.32	0.47	152	-0.56 to 0.19	0.32 to 0.57	140 to 170
1000-1600 AD	0.18	0.70	138	-0.16 to 0.77	0.15 to 0.95	120 to 160
RA 100						
200-1600 AD	-0.33	0.50	154	-0.57 to -0.19	0.36 to 0.60	140 to 170
1000-1600 AD	0.30	0.74	125	-0.19 to 0.87	0.19 to 0.96	70 to 160
Loess 1						
200-1600 AD	-0.32	0.47	154	-0.56 to -0.17	0.44 to 0.57	130 to 180
1000-1600 AD	0.09	0.71	132	-0.37 to 0.69	0.15 to 0.95	70 to 180
Loess 2						
200-1600 AD	-0.32	0.52	161	-0.55 to -0.17	0.38 to 0.64	140 to 190
1000-1600 AD	0.19	0.77	118	-0.41 to 0.88	0.26 to 0.98	50 to 180
Averages						
200-1600 AD	-0.31	0.47	155	-0.54 to -0.09	0.35 to 0.57	140 to 174
1000-1600 AD	0.17	0.70	128	-0.27 to 0.77	0.13 to 0.94	82 to 176

The data in Table 1 and Table 2 reveal the following observations:

1. The original data (Orig) r_{PCC} (max) is consistently lower than the four smoothed transformations (RA 50, RA 100, Loess 1, and Loess2) by about 0.14 (200-1600 AD) and 0.13 (1000-1600 AD). r_{PCC} (0-lag) is lower by about 0.07 (200-1600 AD) and 0.17 (1000-1600 AD). These numbers are from Data Set A. Data Set B shows the same trend with slightly smaller values. However, the Orig r_{PCC} (max)is 0.52 and 0.76, respectively, for the longer and shorter ranges of Data Set A, which are Moderate and Strong correlations. For Data Set B, the Orig r_{PCC} (max) values are 0.41 and 0.59 for the longer and shorter ranges respectively. Thus, the original data, without smoothing and with a larger noise component, still record significant conditional correlation values.
2. The RA 50 series is similar, but the values tend to lie between Orig and RA 100 which is consistent with the gradational nature of increasingly smooth character. The RA 50 r_{PCC} (max) is 0.66 and 0.87, respectively, for the longer and shorter ranges of Data Set A, which are Moderate and Strong correlations. For Data Set B, the RA 50 r_{PCC} (max) values are 0.47 and 0.70 for the longer and shorter ranges respectively.

3. The r_{PCC} values (no lag) vs. the r_{PCC} values (max lag) are always significantly lower for every transformation method, for both data ranges, and for every CO_2-temperature correlation pair. The average differential in Orig r_{PCC} (max) (200-1600 AD) is 0.57 for Data Set A, and 0.65 for Data Set B. The average differential in Orig r_{PCC} (max) (1000-1600 AD) is 0.59 for Data Set A, and 0.51 for Data Set B. The change in correlation strength is from None to Very Strong, thus emphasizing the lack of correlation from a statistical perspective for the no lag case.
4. While the average Orig CO_2 lag to temperature of both Data Sets A and B is about the same for the 200-1600 AD range, 151 and 154 yr respectively, and likewise for the 1000-1600 AD range, 135 and 128 yr, the range of lag is about 100 to 200 yr with a tighter cluster between 130 and 170 yr respectively. For the Orig data the average lag is about 153 yr and 132 yr, respectively, while for the RA 50 data the average lag is about 152 yr and 135 yr, respectively.
5. As shown below in the Original Charts (Fig. 1 and Fig. 2) of CO_2 and temperature, the most likely lag is about 150 yr based on prominent markers. Thus, the conditional r_{PCC} (max) values for Original and RA 150 at the full data range of 200-1600 AD (156 and 152) seem to be a close match to the physical chart of the data even with a higher degree of noise component.
6. Observations regarding the shorter and younger range of 1000-1600 AD versus the longer range of 200-1600 AD:
    6.1. r_{PCC} (max) lagged data for 1000-1600 AD has a consistently higher r_{PCC} average differential of 0.23 compared to the 200-1600 AD range.
    6.2. While all of the r_{PCC} values of the data with no lag are very low, 200-1600 AD is consistently lower than 1000-1600 AD: 0.07 at 0.47.
    6.3. The CO_2 lag to temperature is recoding about 23 yr higher for the longer range than the shorter range.
    6.4. The r_{PCC} correlations may be somewhat lower for the 200-1600 AD period, although still showing at least Moderate strength of correlation, due to a probable lower sampling rate by the various researchers in the range of 1-1000 AD. Also, the Little Ice Age (LIA) is identified as ranging from 1300-1850 AD (Mann et al., 1999), but as shown in Fig. 1, temperature begins to steeply decline around 1100 AD and completes its rebound around 1900 AD. The dynamics of the LIA may have been a factor.
7. Running Average (RA 100) with significantly lower smoothing factor than Loess1 or Loess2, records similar r_{PCC} values for the respective ranges of 200-1600 AD and 1000-1600 AD.
8. It is observed the r_{PCC} for the longer range, ≈ 200 to 1600 AD, is always a bit lower than the r_{PCC} for the shorter range (Table 1). There are several possible reasons for this result. The data sample distribution in most of the published studies was sparser in the years below 1000 AD. Having a longer-range extent will possibly introduce more inaccuracy and less precision. It is possible the driving process responsible for the 150-yr lag of CO_2 to temperature may fluctuate somewhat over time.
9. Loess 2 appears to show the highest r_{PCC} compared to the other transformations.
10. Generally, regarding the different sources of data, there does not appear to be a significant difference among the CO_2 data sources or the temperature data sources with this view of the data. Two or three of the temperature sources in Data Set B do appear to be somewhat out of phase with the rest of the temperature data, although the major trends appear intact.
11. Given the influence of smoothing, preprocessing, and probable auto-correlation (Long-term memory), these r_{PCC} correlations should be viewed as context-dependent indicators

rather than fixed or universal measures of the CO_2–temperature relationship. They should be interpreted comparatively rather than as intrinsic measures. The Statistical Validation Process described in Supplementary Material, Appendix B, should provide guidance as to whether the correlation analysis of individual pairs be considered significant.

3.2 Statistical Validation Framework (SVF) Summary

Given the well-documented concerns regarding autocorrelation, long-range dependence (LRD), and smoothing-induced bias in paleoclimate time series, a dedicated Statistical Validation Framework (SVF) was developed and applied to all Pearson correlation results in this study. The SVF combines multiple diagnostic tests to safeguard against false-positive inferences and ensures that any reported associations between CO_2 and temperature meet rigorous statistical thresholds.

As outlined in the Methods section and detailed fully in Supplementary Material, Appendix B, the SVF includes seven validation categories: (1) autocorrelation testing (Durbin-Watson (Durbin & Watson, 1950), Breusch-Godfrey (Breusch, 1978; Godfrey, 1978), and Ljung-Box (Ljung & Box, 1978)); (2) Hurst exponent analysis using R/S, DFA, and GPH methods; (3) HAC (Heteroskedasticity and Autocorrelation Consistent) standard errors; (4) estimation of the effective sample size (Neff); (5) block permutation testing; (6) false discovery rate (FDR) correction; and (7) final significance classification based on joint criteria. The goal of the SVF is not to suppress correlation results but to distinguish robust signal from statistical artifact in the presence of serial correlation and LRD — concerns highlighted by Koskinas et al. (2022), Koutsoyiannis (2024c), and others.

Out of 64 primary CO_2–temperature pairs evaluated (across multiple lags and smoothing levels), 79 of 320 pairings passed at least one SVF statistical significance threshold, with Neff $\geq$ 10 or Neff $\geq$ 8. Most statistically reliable results (r_{PCC} passing all SVF tests) occurred in unsmoothed or lightly smoothed datasets — especially the Original and Running Average 50 (RA 50) CO_2 series. A smaller number of valid results emerged from RA 100 and Loess-smoothed datasets, though these were treated with caution due to inflation risk. These outcomes reinforce the overall finding that correlation strength alone is not sufficient to infer significance without correcting for structural dependencies.

In order to reduce serial dependence and improve the reliability of statistical inference, all correlation analyses were performed on down-sampled series. All pairs were down-sampled by five subsets (every $1/10^{th}$, $1/20^{th}$, $1/30^{th}$, $1/40^{th}$, and $1/50^{th}$). Final selection of unique pairs was based on Neff value, down-sampling, and n (final sample size), and to some degree r_{PCC}. Some pairs required more aggressive down-sampling depending on autocorrelation structure and overall series length. While down-sampling helps mitigate inflation of r_{PCC} due to autocorrelation, it can also reduce the number of observations (n) available for correlation. To preserve meaningful statistical power, the final selection of unique, SVF-passing pairs balanced multiple criteria — including correlation strength (r_{PCC}), effective sample size (Neff), and actual sample count (n) as shown in Table B4, Supplementary Material, Appendix B. In a few cases, a slightly smaller Neff value was accepted in favor of a higher n value, provided all SVF thresholds were still satisfied. This conservative approach prioritized statistical validity while ensuring that results were not driven by overly small sample sizes.

Later, sections of this paper will visually display selected CO_2–temperature pairs using smoothed Loess curves for interpretive clarity, but will explicitly annotate on each figure whether the underlying pair passed SVF criteria in its Original or RA 50 form. A summary comparison chart showing Original, RA 50, and Loess curves will also be provided to highlight their structural similarity and justify visual interpretation. In this way, SVF results are fully transparent and integrated, allowing readers to assess both statistical and visual coherence across all candidate relationships.

3.3 Structural Break or Regime Shift in the CO_{2Lag} and Temperature Data at 1600 AD

Unexpected behavior across the boundary of 1600 AD in the CO_{2Lag} and temperature data, prompted testing for stability or non-stationarity in the CO_2–temperature relationship. Therefore, formal structural break analysis centered on 1600 AD was conducted. This breakpoint was hypothesized based on a marked reduction in correlation when extending from the 200–1600 AD segment to the full 200–1850 AD range. It is also about the time period where CO_{2Lag} accelerated higher exponentially; temperature accelerated higher; and the nadir of the Little Ice Age occurs. Supplementary Material, Appendix C, details the application of three diagnostic tests: (1) the Chow test for structural discontinuity (Chow, 1960), (2) segmented Pearson correlation analysis, and (3) regression slope comparison across pre- and post-1600 intervals. Results show a highly significant F-statistic ($F = 877.23$) and an ~87% drop in regression slope post-break, alongside the collapse of full-span correlation ($r \approx -0.06$). These findings collectively indicate either a statistical phenomenon (structural break) or a large ecosystem change (regime shift) in system dynamics at 1600 AD, warranting the partitioning of subsequent analyses into distinct temporal phases. A detailed discussion with test results, about the structural break or regime shift, is presented in Supplementary Material, Appendix C.

3.4 Data Results - CO_2 vs. Temperature (1600-1850 AD)

The data within the range of 1600-1850 AD was analyzed separately due to three previous outcomes:

1. The analysis of the entire range of CO_2 and temperature data from 200-1850 AD
2. The evidence of a structural break or regime shift in the data at 1600 AD shown in section 3.2
3. The analysis of the range of data from 200-1600 AD as shown in section 3.1

A more robust correlation analysis approach was conducted with one transformation level of the data, Running Average (50-yr centered). This was due to the structural break condition at about 1600 AD and the exceptional steep trending slopes of both CO_2 and temperature after 1600 AD. This approach calculated the following (Table A23 in Supplementary Material, Appendix A):

1. r_{PCC} (no lag of CO_2 to temperature)
2. r_{PCC} (maximum r_{PCC}) (calculated from -100 to +250 lag years in 5 yr intervals)
3. lag (lag interval with the maximum r_{PCC})
4. Averages of each calculated parameter per CO_2 and temperature source

Three CO_2 sources and 6 temperature sources were utilized from this study.

The following steps were followed in deriving the results:

1. Cubic Transformation of CO_2 to enhance sensitivity to relative increases (Hyndman & Athanasopoulos, 2018).
2. The cubed CO_2 series was linearly detrended to remove long-term trends and better isolate internal variability (Granger & Newbold, 1974: Box et al., 2015).
3. Normalization of both CO_2 and temperature using min-max scaling to enable direct comparison. This technique facilitates comparative analysis, particularly when applying regression-based methods across differently scaled data (James et al., 2021).
4. Smoothing via a 50-yr Running Average to reduce high frequency variability. In correlation metrics smoothing improves stability while preserving decadal patterns of climate variability (von Storch & Zwiers, 1999).
5. Lag-alignment of CO_2 to temperature was calculated utilizing a lag range of -100 to 250 yr in 5-yr increments to determine the lag of the highest r_{PCC} value. This both identifies the

lag and tests the hypothesis of a CO_2 to temperature of about 150 yr as observed with the data from 200-1600 AD (Granger, 1969; Mudelsee, 2010).

6. Pearsons Correlation Coefficients were calculated conditionally, in the same manner as for the data range of 200-1600 AD, since autocorrelation and long-term memory are issues that could inflate r_{PCC} somewhat (Beran, 1994).

The data in 1600-1850 AD is similar to the range of 200-1600 AD in that it is autocorrelated and exhibits evidence of long-memory behavior, however based on the previous analysis shown in Supplementary Material, Appendix A, use of r_{PCC} is considered conditionally acceptable for this study.

Referring to Table A23, in Supplementary Material, Appendix A, there are a few observations made for this RA 50 smoothing level data:

1. The average correlation is 0.85 at an average lag of 199 yr (range 130-250). This is a Very Strong correlation.
2. The average correlation is 0.29 at No Lag, indicating the hypothesis of CO_2 lagging temperature by about 150 yr is strong, and not the reverse, as popularly hypothesized.
3. The strongest lagged relationship is observed between the Juckes temperature series and Ahn CO_2 data (r_{PCC} = 0.99 at a lag of 210 yr).
4. Based on the data alone, it appears the relationship of CO_2 to temperature is not significantly different between the two ranges of data (200-1600 AD and 1600-1850 AD), even with the structural break at 1600 AD. CO_2 lags temperature by at least 150 yr, which effectively places all of the CO_2 data to present day as influenced centennially by temperature about 150 ys in the past.

3.5 Graphical Results - Original CO_2 and Temperature (200-1600 AD)

Visual and correlation analysis of CO_2 versus temperature results are presented utilizing many of the widely recognized studies of CO_2 and temperature covering the past 2000 yr.

Conditional correlation analysis in the form of r_{PCC} has been conducted on all of the data analyzed, and all 5 forms including the Original data (Orig), Running Average (RA 50); Running Average (RA 100); Loess 1 (lesser smoothing algorithm); and Loess 2 (greater smoothing algorithm). Maximum r_{PCC} – lag analysis was also conducted and results are shown on Tables A1 through A22 in Supplementary Material, Appendix A.

As discussed in detail in the Supplementary Material, Appendix B, a robust statistical analysis, Statistical Validation Framework (SVF), has been conducted on all data in this study, and roughly 25% of the r_{PCC} pairs passed statistical significance at either Robustly Significant or Tentatively Significant. Thus, all of the charts shown will identify this status. In many cases a chart will be presented at a higher smoothing factor, which itself has not passed the SVF, but one of its other variants has, and this status will be identified. For example, a Loess 2 chart may be shown (not passed), but it is a smoothed variant of an Orig or RA 50 that has passed the full SVF, meeting all criteria. Rather than formal inference, the purpose of the Loess 2 Chart would be to present an enhanced visual expression of the validated version illustrating the temporal and structural alignment in a visually compelling manner, not necessarily introducing an entirely new relationship. In these cases, the Loess 2 chart would be labelled as "conditional", based on the corresponding Orig or RA 50 SVF pass status. This illustrates that while high smoothing can visually enhance apparent alignment, formal inference must rely on statistical validation. This is consistent with best practices in statistical communication, where exploratory or supporting plots are distinguished from validated results (Kauffman et al., 2020; McGregor et al., 2013; Tufte, 2001; Gelman & Hill, 2006).

Fig. 1 shows a good example of the original data of CO_2 (Rubino et al., 2019) plotted against the

original data of temperature (Ljungqvist, 2010) from about 1 to 2000 AD. Upon inspection, even with a noise component, it is apparent the two curves visually correlate very well with each other, but only if the CO_2 curve is time-shifted 150 yr earlier to correct for the CO_2 lag. Both the original CO_2 curve and the shifted CO_2 curves reflecting the lag are shown in the figure.

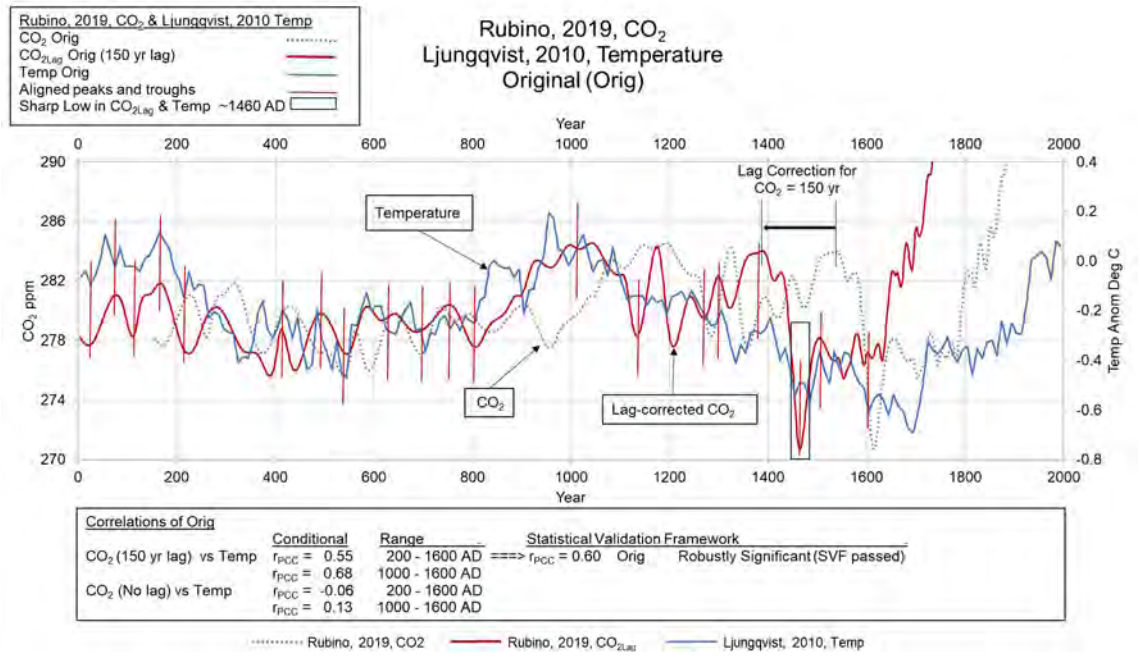

Figure 1. Original CO_2 and temperature data (from Rubino et al., 2019; Ljungqvist, 2010, respectively) are shown from 1 to 2000 AD along with the CO_2 curve shown with a 150-yr lag correction. Aligned peaks and troughs are depicted with thin red lines. A sharp low in CO_{2Lag} and temperature are shown at about 1460 AD. r_{PCC} is shown for lagged 150 yr and no lag for both ranges of 200-1600 AD and 1000-1600 AD. Orig for this pair is directly validated under SVF, and its correlation is presented here conditionally, supported by the corresponding result, Robustly Significant (SVF passed). The complete list of SVF passed pairs is in Supplementary Material, Appendix B, Table B4.

Visual correlations covering peaks and troughs of 50-100 yr as well as 800-1000 yr are observed between the two curves of CO_{2Lag} and temperature. Aligned peaks, or peak-clusters, are observed at about 80, 175, 410, 490, 590, 740, 920-1100, 1240, 1300, 1360-1420, and 1500-1575 AD. Correlative troughs can also be observed, in particular, the deep trough at about 1460 AD. At this year, with close precision, a deep trough is identified on almost every CO_{2Lag} and temperature pair analyzed in this study.

At about 1775 AD for CO_2 and 1625 AD for CO_{2Lag}, the CO_2 curves take a sharp and exponentially high shift probably coinciding with the temperature curve which begins to increase more steeply, but at a much lower slope than CO_2. The Little Ice Age spanning from about 1100-1300 AD to about 1900 AD shows its latter upward temperature recovery from about 1700 to about 1900 AD, as it moves out of the low point of the Little Ice Age.

Fig. 1 also shows two broad trends of temperature: (1) peaks at about 100 AD and about 1000 AD with a trough at about 500 AD, and (2) peaks at about 1000 AD and about 2000 AD with a trough at about 1500 AD. These features may be associated with the 1000-yr cyclicity of earth climate indices and solar activity -- Eddy Cycle (Zhao et al., 2020). While there is not adequate length of data in the temperature records presented here to define a cycle of that nature, the amount of data that is present is consistent with the proposed, but not proven, Eddy cycle. However, below in this article, data is presented showing relative correlation between the temperature data curves and Total Solar Irradiance.

Fig. 2 shows the original data of CO_2 from (Rubino et al., 2019) plotted against the original data

of temperature from Moberg et al. (2005) for the same period in the last 2000 yr. Similar to Fig. 1, the CO_2 curve and temperature curve in Fig. 2 correlate visually only when the CO_2 curve is shifted 150 yr.

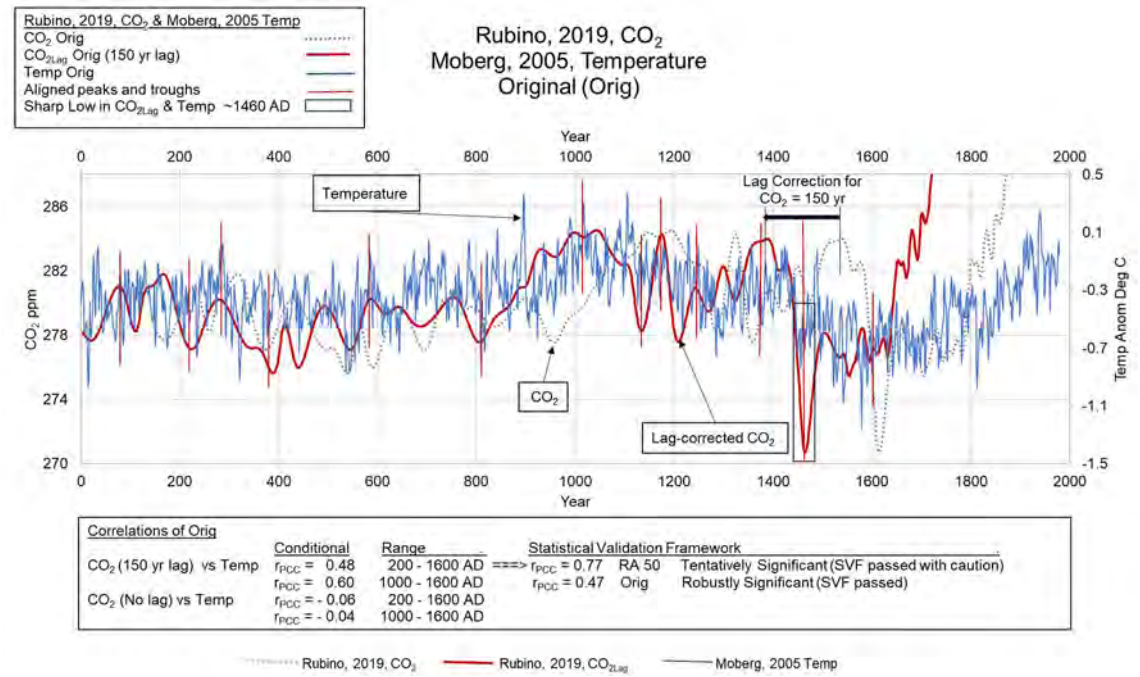

Figure 2. Original CO_2 and temperature data (from Rubino et al., 2019; Moberg, 2005, respectively) are shown from 1 to 2000 AD along with the CO_2 curve shown with a 150-yr lag correction. Aligned peaks and troughs are depicted with thin red lines. A sharp low in CO_{2Lag} and temperature are shown at about 1460 AD. r_{PCC} is shown for CO_2 lagged 150 yr and no lag for both ranges of 200-1600 AD and 1000-1600 AD. Orig for this pair is directly validated under SVF, and its correlation is presented here conditionally, supported by the corresponding result, Robustly Significant (SVF passed). The variant, RA 50, is also SVF-validated at Tentaatively Significant, passed with caution. The complete list of SVF passed pairs is in Supplementary Material, Appendix B, Table B4.

While evaluating the original published data included in Fig.1 and Fig. 2, even with a high noise-level component, certain key common observations can be made:

1. The CO_{2Lag} of about 150 yr with temperature, is consistent and representative of all 64 original pairs of CO_2 versus temperature data in this study.
2. The CO_{2Lag} curve is interrupted by a shift in the CO_2 curves at about 1600 AD (1750 AD on the CO_2 non-lagged curve). While CO_2 accelerates rapidly from this point, temperature climbs, but at a lower rate. This observation is consistent with all 64 data correlations.
3. Many peaks and troughs, and peak-trough clusters, of varying widths from 10 yr to 150 yr, appear to visually correlate between the CO_{2Lag} and temperature curves.
4. There is a sharp notched decline of both CO_{2Lag} and temperature at about 1460 AD with a width of 50 yr to 80 yr. This distinctive feature appears as a signature marker on all 64 correlations of CO_{2Lag} and temperature.
5. A potential long cycle is observed on the temperature curves (shadowed by the CO_{2Lag} curves) with peaks at about 100, 1000, and 2000 AD, and troughs at about 550 and 1500 AD, with a frequency cycle of about 1000 yr. This appears to very closely shadow the proposed Eddy Cycle for this range of data (Zhao et al., 2020). A longer data record showing these repeatable features with several major peaks and troughs would be desirable.

3.6. Graphical Results - Smoothed CO_2 and Temperature (200-1600 AD)

Fig. 3 presents five curves representing all smoothing transformation variants for a specific temperature series, (Hegerl, 2007), which shows the degree of variation in the charted curves typical of all of the series in the study. The Orig (violet) curve is the original published data which generally has more noise. However, this curve retains the sharper peaks and troughs which represent key markers, such as the marker at 1460 AD which is observed on almost all of the curves in this study: CO_{2LAG} at 150 yr, temperature, and Total Solar Irradiance (TSI). The RA 50 (black) curve is the least-smoothed of the transformed curves, but retains the major peaks and troughs while shedding the minor noise. The RA 100 (red) curve is often very close to the Loess 1 (green) curve in character, and maintains the more major peaks and troughs while shedding the minor ones. The Loess 2 (blue) curve is the most smoothed, and generally reflects the more regional trends, while it smooths away the noise and smaller more granular features.

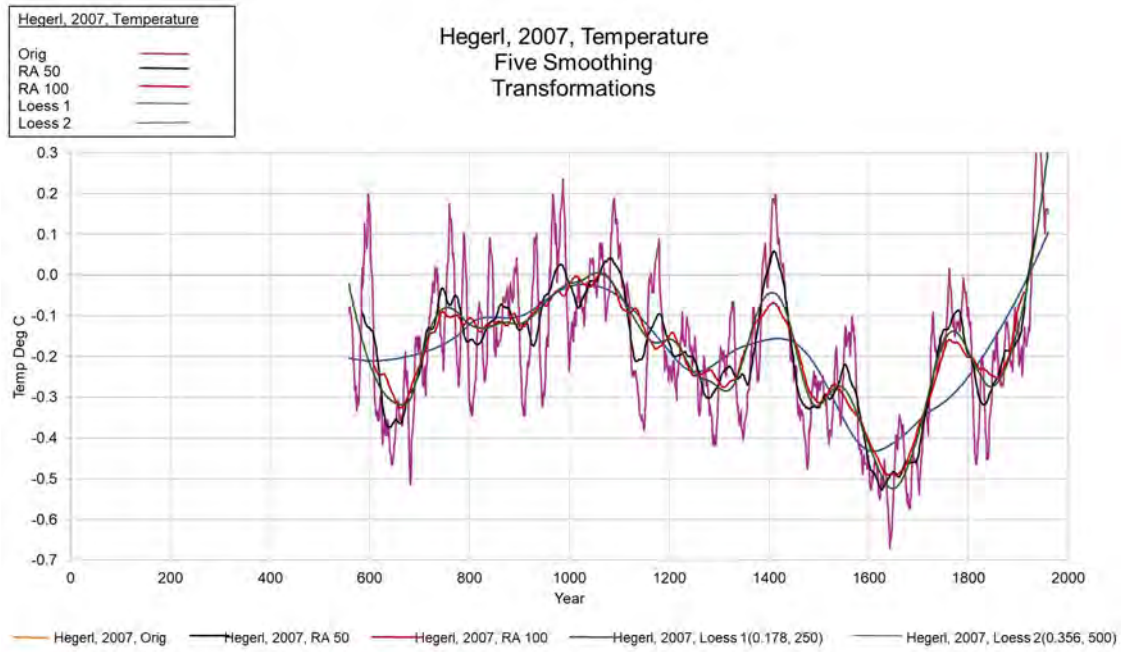

Figure 3. Presents five forms of the temperature series, Hegerl et al., 2007: Original published data, Orig; Running Average centered on 50 yr, RA 50; Running Average centered on 100 yr, RA 100; smoothing algorithm, Loess 1 (Loess, 0.178, 250); and smoothing algorithm, Loess 2 (Loess, 0.356, 500).

As displayed below in Fig. 4, on the Running Average (RA 50) chart, the visual correlation is excellent for the two curves — (1) Ljungqvist (2010) temperature (blue) and (2) Rubino et al. (2019) CO_{2Lag} (red). The CO_{2Lag} curve is time-shifted 150 yr earlier to correct for the lag. This is shown by the curves tracing each other from 200 to 1600 AD. The original CO_2 curve represented by a dashed light gray curve is clearly out of synch with the temperature curve. Several thin vertical red lines are drawn to highlight close orientation of many of the peaks and troughs showing more granular alignment. The general curvature aligned between the two curves over 2000 yr is easily apparent. From 1600 AD to about 1850 AD, the lagged-CO_2 and temperature curves also track on steep inclinations with CO_{2lag} having a slightly steeper slope. Similar to the Original curves in Fig. 1, the visual correlation is excellent as are the conditional r_{PCC} correlation numbers. For the data range 1000-1600 AD the r_{PCC} is stronger. The comparison of the CO_{2Lag} vs. no lag is striking with r_{PCC} showing 0.81 and 0.28 for the data range of 1000-1600 AD and 0.67 and 0.06 for the data range of 200-1600 AD. This sharp differential of Strong correlation to No correlation agrees with the visual inspection of the chart where CO_2 is clearly offset by 150 yr. The running average smoothing, centered at 50 yr (RA 50), allows easier visual review than Orig, while the smoothing modifies the curve only slightly by removing noise, smaller inflections, and localized features. Although RA 50 smoothing for this pair is not directly validated under SVF, its

correlation is presented here conditionally, supported by the corresponding Orig variant which passed full SVF criteria for statistical significance with Robustly Significant (SVF passed). The complete list of SVF passed pairs is in Supplementary Material, Appendix B, Table B4.

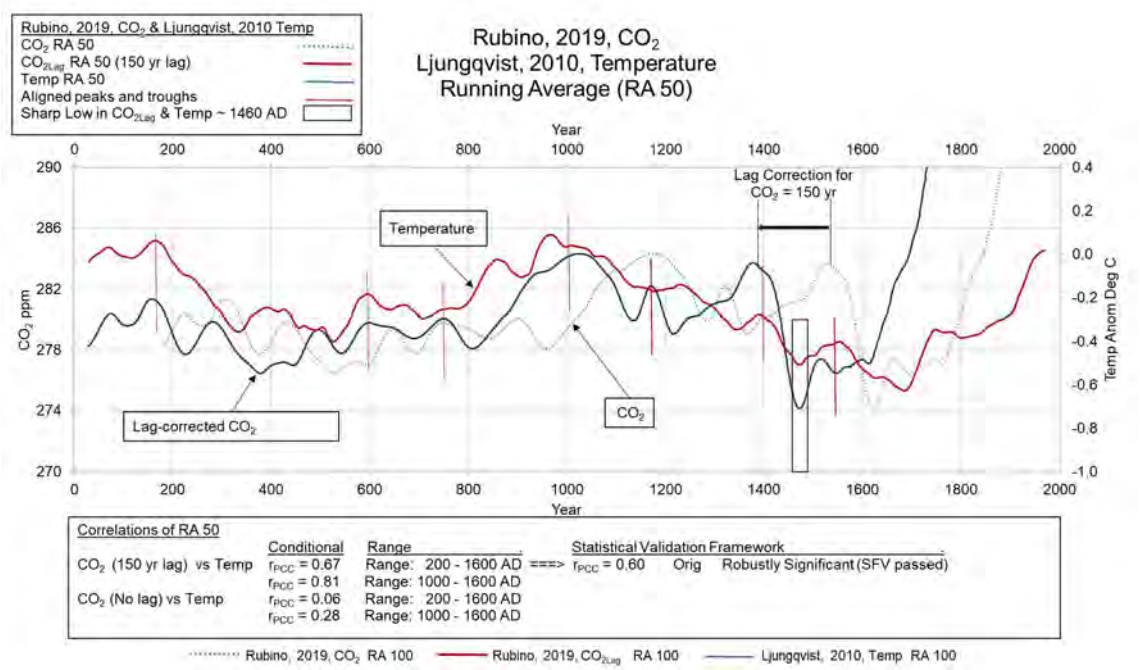

Figure 4. Running Average smoothing, centered 50 yr, (RA 50), CO_2 and temperature data (from Rubino et al., 2019; Ljungqvist, 2010, respectively) are shown from 1 to 2000 AD along with the CO_2 curve shown with a 150-yr lag correction. Aligned peaks and troughs are depicted with thin red lines. r_{PCC} is shown for 150-yr lag and no lag for both ranges of 200-1600 AD and 1000-1600 AD. Although RA 50 smoothing for this pair is not directly validated under SVF, its correlation is presented here conditionally, supported by the corresponding Orig variant which passed full SVF criteria for statistical significance with Robustly Significant (SVF passed). The complete list of SVF passed pairs is in Supplementary Material, Appendix B, Table B4.

Another excellent example of visual correlation is a chart showing RA 100 smoothing with a Very Strong r_{PCC}, as observed in Fig. 5. Several thin vertical red lines are drawn to highlight key peaks and troughs. In this chart, Rubino et al. (2019) is compared to Yang et al. (2002). The continuous alignment over the 2000 yr is striking when comparing the temperature (blue) to CO_{2Lag} (red) curves. The CO_{2Lag} curve is corrected 150 yr from its original position shown by CO_2 (dotted gray). From 1600 AD to about 1850 AD, the lagged-CO_2 and temperature curves also track on steep inclinations with CO_{2lag} having a slightly steeper slope. This is similar as observed in Fig. 4. For the data range, 1000-1600 AD, the r_{PCC} is stronger. The comparison of the CO_{2Lag} vs. no lag is impressive with r_{PCC} showing 0.93 and 0.15 for the data range of 1000-1600 AD and 0.72 and 0.13 for the data range of 200-1600 AD. The Very Strong correlation to Weak correlation agrees with the visual review of the chart where CO_2 is clearly offset by 150 yr. Comparisons of r_{PCC} should be considered conditional, as mentioned previously. Even though RA 100 is not directly validated under SVF, Orig and RA 50 for this pair are both directly validated, and the r_{PCC} correlation is presented here conditionally, supported by the corresponding result, Robustly Significant (SVF passed). Smoothing visually enhances apparent alignment, but should be statistically validated for formal inference. The complete list of SVF passed pairs is in Supplementary Material, Appendix B, Table B4.

Loess smoothing was applied to all pairs of CO_2 and temperature as well as all pairs of CO_{2Lag} and temperature in this study. Two levels of Loess were applied, somewhat subjectively. Loess 1 tends to be close to RA 100, while Loess 2 is smoother, and tends to eliminate more local features, accentuating the larger-scale features.

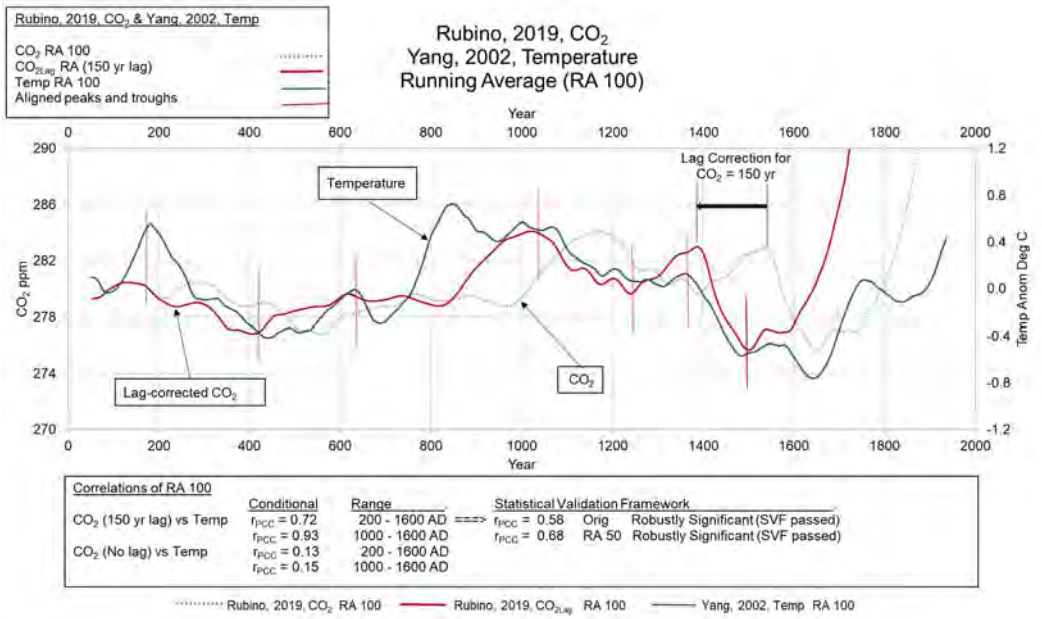

Figure 5. Running Average smoothing, 100 yr, centered, CO_2 and temperature data (from Rubino et al., 2019; Yang et al., 2002, respectively) are shown from 1 to 2000 AD along with the CO_2 curve shown with a 150-yr lag correction. Aligned peaks and troughs are depicted with thin red lines. r_{PCC} is shown for CO_2 lagged 150 yr and no lag for both ranges of 200-1600 AD and 1000-1600 AD. Although RA 100 is not directly validated under SVF, Orig and RA 50 for this pair are both directly validated, and the r_{PCC} correlation is presented here conditionally, supported by the corresponding result, Robustly Significant (SVF passed). Smoothing visually enhances apparent alignment, but should be statistically validated for formal inference. The complete list of SVF passed pairs is in Supplementary Material, Appendix B, Table B4.

As discussed previously, r_{PCC} is used conditionally in this study due to autocorrelation and long-memory issues, although mitigated with various tests and methods (SVF). It should be noted that one of the concerns with autocorrelation and long-memory is an inflation of r_{PCC}, which is exhibited in the data, where r_{PCC} is increasingly larger from Original to RA 100 to Loess 1 to Loess 2. However, visually comparing the curves where higher r_{PCC} values are found does show commensurately closer visual correlation. Comparing the relative values of a maximum r_{PCC} at an observed lag for CO_{2Lag} against r_{PCC} for the no lag case will not be an issue. It subjectively appears that the increase in r_{PCC} as additional smoothing is applied, for the data in this study, is due to a combination of the two factors—some inflation due to autocorrelation and long memory effects and a resulting closer correlation for the broader more regional aspect. In either event the approach discussed previously in applying a battery of statistical tests associated with the Statistical Validation Framework appears to add confidence to using the r_{PCC} data more quantitatively when the correlated pairs pass either as Robustly Significant (SVF passed) or Tentatively Significant (SVF passed with caution) (in Supplementary Material, Appendix B, Table B4).

Four typical examples of smoothed data are shown respectively in Fig. 6, based on Loess 2 smoothed data by Rubino et al. (2019) and Ljungqvist (2010), Fig. 7, based on Loess 2 smoothed data by Rubino et al. (2019) and Yang et al. (2002), Fig. 8, based on Loess 2 smoothed data by MacFarling Meure et al. (2006) and Hegerl et al. (2007), and Fig. 9, MacFarling Meure et al. (2006) and Yang et al. (2002). The smoothed curves show a very close visual relationship between CO_{2Lag} and temperature. Large scale rolling peaks and troughs exhibit strong visible correlation, and the conditional correlation r_{PCC} values are Very Strong as labelled on the figures. The CO_{2Lag} curves have both been corrected by 175 (Fig. 6), 150 (Fig. 7), 120 (Fig. 8), and 150 (Fig. 9) yr for CO_2 lag, respectively, as indicated by correlation analysis as a function of lag correction (Tables A9 and A10, Supplementary Material, Appendix A).

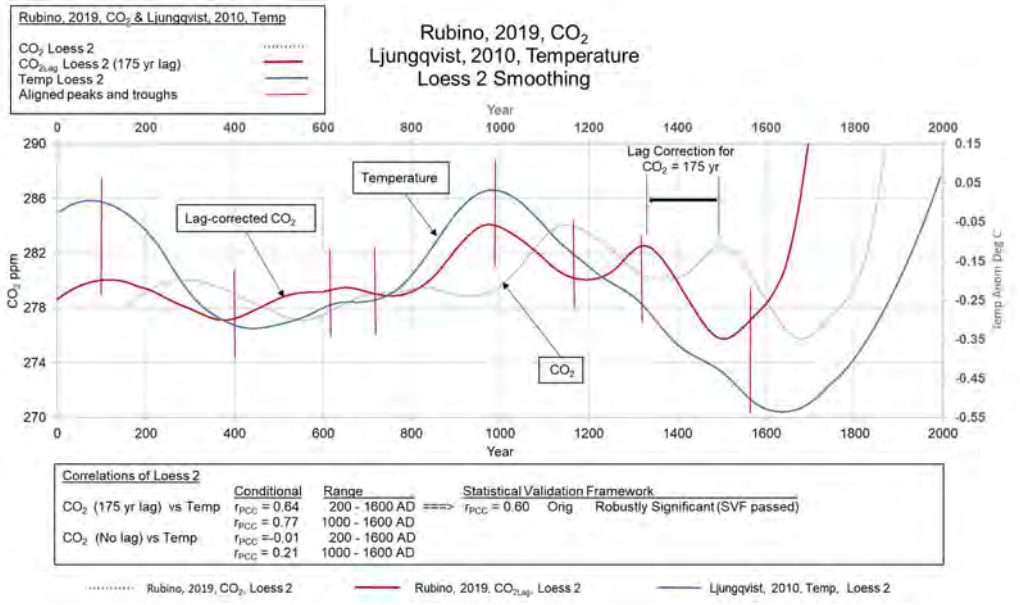

Figure 6. Loess 2 smoothing, CO_2 and temperature data (from Rubino et al., 2019; Ljungqvist, 2010, respectively), are shown from 1 to 2000 AD along with the CO_2 curve shown with a 175 yr lag correction. Aligned peaks and troughs are depicted with thin red lines. r_{PCC} is shown for CO_{2Lag} lagged 175 yr and no lag for both ranges of 200-1600 AD and 1000-1600 AD. Although Loess 2 smoothing for this pair is not directly validated under SVF, its correlation is presented here conditionally, supported by the corresponding Orig variant which passed full SVF criteria for statistical significance with Robustly Significant (SVF passed). High smoothing visually enhances apparent alignment, but should be statistically validated for formal inference. The complete list of SVF passed pairs is in Supplementary Material, Appendix B, Table B4.

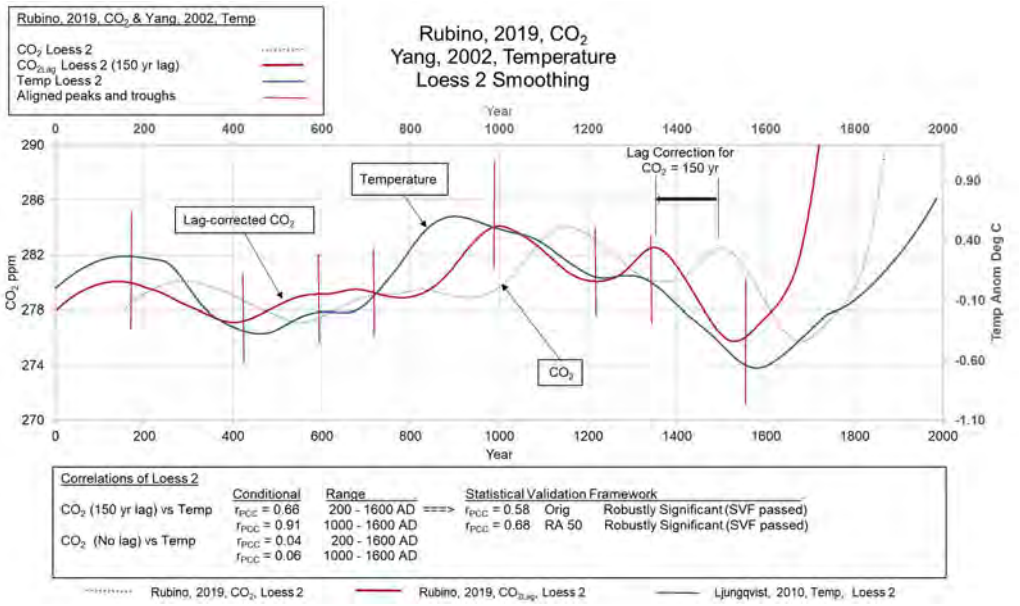

Figure 7. Loess 2 smoothing, CO_2 and temperature data (from Rubino et al., 2019; Yang et al., 2002, respectively), are shown from 1 to 2000 AD along with the CO_2 curve shown with a 150-yr lag correction. Aligned peaks and troughs are depicted with thin red lines. r_{PCC} is shown for CO_{2Lag} lagged 150 yr and no lag for both ranges of 200-1600 AD and 1000-1600 AD. Although Loess 2 smoothing for this pair is not directly validated under SVF, its correlation is presented here conditionally, supported by the corresponding Orig and RA 50 variants which passed full SVF criteria for statistical significance with Robustly Significant (SVF passed). High smoothing visually enhances apparent alignment, but should be statistically validated for formal inference. The complete list of SVF passed pairs is in Supplementary Material, Appendix B, Table B4.

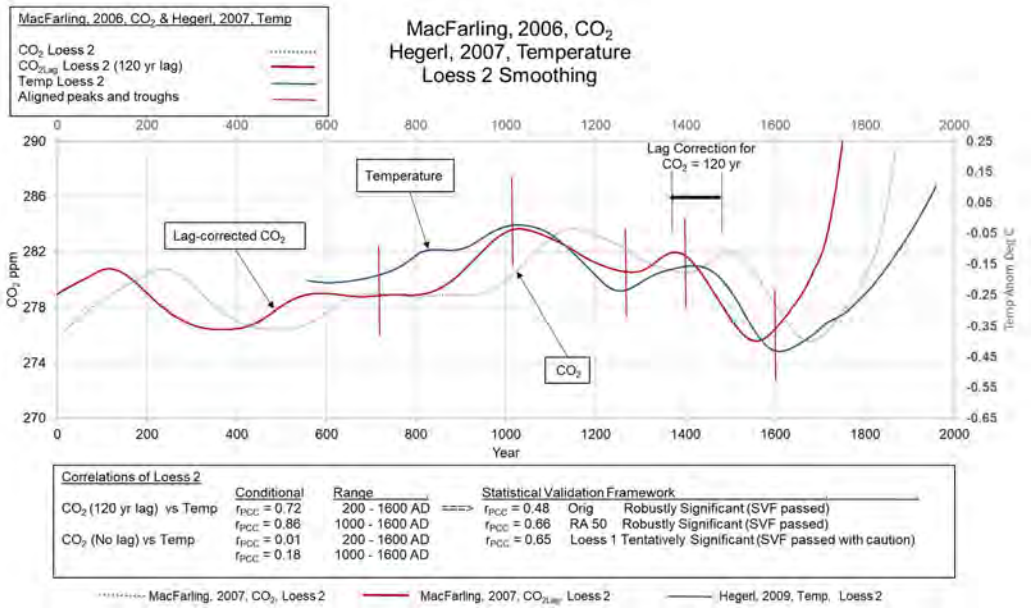

Figure 8. Loess 2 smoothing, CO_2 and temperature data (from MacFarling Muere et al., 2006; Hegerl et al., 2007, respectively), are shown from 1 to 2000 AD along with the CO_2 curve shown with a 120-yr lag correction. Aligned peaks and troughs are depicted with thin red lines. r_{PCC} is shown for CO_{2Lag} lagged 120 yr and no lag for both ranges of 200-1600 AD and 1000-1600 AD. Although Loess 2 smoothing for this pair is not directly validated under SVF, its correlation is presented here conditionally, supported by the corresponding Orig and RA 50 variants which passed full SVF criteria for statistical significance with Robustly Significant (SVF passed). Its correlation is also supported by the corresponding Loess 1 variant which passed SVF criteria for statistical significance with Tentatively Significant (SVF passed with caution). High smoothing visually enhances apparent alignment, but should be statistically validated for formal inference. The complete list of SVF passed pairs is in Supplementary Material, Appendix B, Table B4.

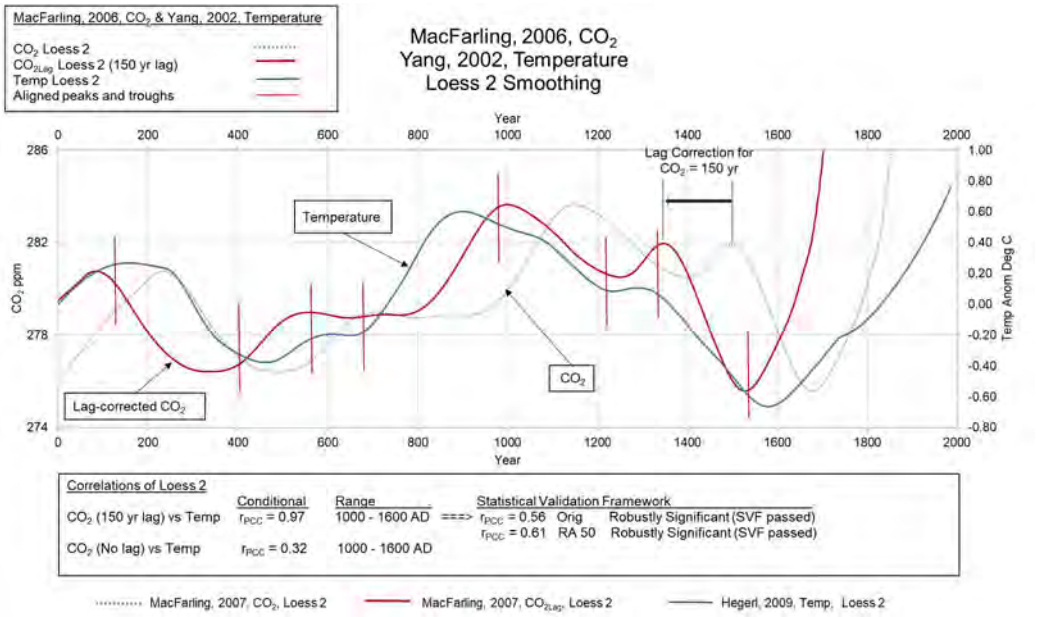

Figure 9. Loess 2 smoothing, CO_2 and temperature data (from MacFarling Meure et al., 2006; Yang et al., 2002, respectively), are shown from 1 to 2000 AD along with the CO_2 curve shown with a 150-yr lag correction. Aligned peaks and troughs are depicted with thin red lines. r_{PCC} is shown for CO_{2Lag} lagged 150 yr and no lag for both ranges of 200-1600 AD and 1000-1600 AD. Although Loess 2 smoothing for this pair is not directly validated under SVF, its correlation is presented here conditionally, supported by the corresponding Orig and RA 50 variants which passed full SVF criteria for statistical significance with Robustly Significant (SVF passed). High smoothing visually enhances apparent alignment, but should be statistically validated for formal inference. The complete list of SVF passed pairs is in Supplementary Material, Appendix B, Table B4.

On all four charts (Fig. 6, Fig. 7, Fig. 8, and Fig. 9) at about 1600 AD show an exponential rate of increase in CO_{2Lag} and temperature, as does the corresponding CO_2 curve at about 1750 AD, whereas the temperature curve depicts a much smaller rate of increase. All four charts identify with one to two variant curves that have passed the SVF as Robustly Significant, while one chart added a third pass, Tentatively Significant, passed with caution. High smoothing visually enhances apparent alignment, but should be statistically validated for formal inference as thes charts signify. The complete list of SVF passed pairs is in Supplementary Material, Appendix B, Table B4.

Fig. 10 presents another chart of CO_2, CO_{2Lag}, and temperature with pairs at Loess 2 with a 130-yr lag of CO_{2lag}. This particular pair had three variants of which two have Robustly Significant (SVF passed) variants, Orig and RA 50. The other variant, RA 100, is Tentatively Significant (SVF passed with caution). The visual correlation is quite good, substantiating the r_{PCC} and SVF results. This chart includes Rubino et al. (2019) CO_2 data and Hegerl et al. (2007) temperature data with excellent visual correlation and commensurate correlation data.

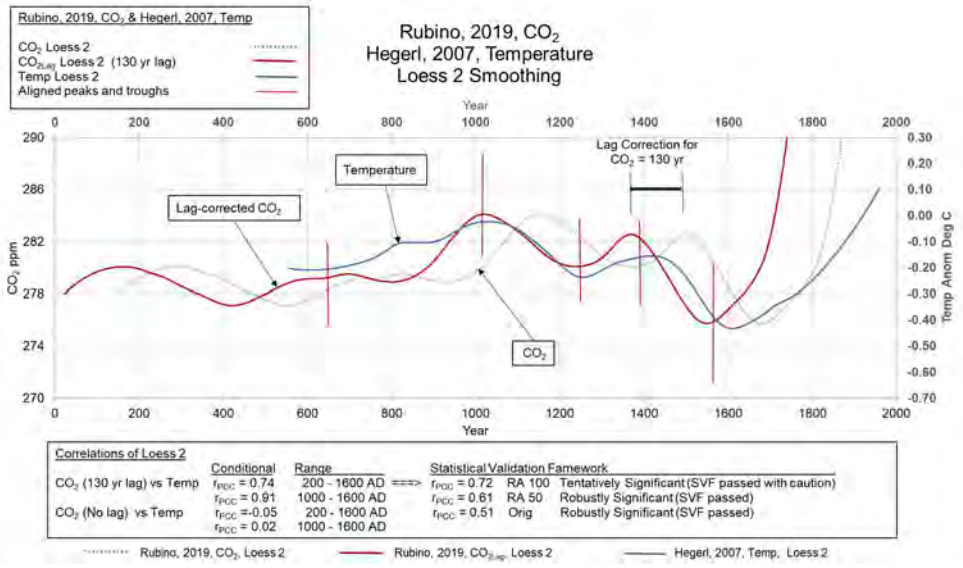

Figure 10. Loess 2 smoothing, CO_2 and temperature data (from Rubino et al., 2019; Hegerl et al., 2007, respectively), are shown from 1 to 2000 AD along with the CO_{2Lag} curve shown with a 130-yr lag correction. Aligned peaks and troughs are depicted with thin red lines. r_{PCC} is shown for both analyzed ranges of 200-1600 AD and 1000-1600 AD. Although Loess2 for this pair is not directly validated under SVF, its correlation is presented here conditionally, supported by the corresponding variants RA 100, Tentatively Significant (SVF passed with caution), and RA 50 and Orig, both Robustly Significant (SVF passed).

In summary, the graphical results for smoothed CO_2 and temperature data in the overall range of 200-1600 AD in this study, show a strong and reproducible visual correlation between temperature and CO_2 when it is CO_2 lag-corrected by about 150 yr. This relationship is consistent and continuous over the entire period and can be observed with the original published data and every variant tested (RA 50, RA 100, Loess 1, and Loess 2) for all combinations of 4 CO_2 series and 16 temperature series. Several combinations of CO_2 and temperature series are displayed the figures in this section of the report to show the consistency of correlation across the different published data.

Pearson's Correlation Coefficient was calculated for all pairs and variants as shown above, and with the confirmation of a significant number of pairs passing a rigorous Statistical Validation Framework process (in Supplementary Material, Appendix B), confidence can be placed in the results.

Although data was not included in this section above 1600 AD due to the structural break or regime shift discussed in Section 3.3, data results for range 1600-1850 are presented in Section

3.4, and graphical results for that data range are presented in Section 3.8.

3.7 Graphical Results – Smoothed Average CO_2 and Temperature (200-1600 AD)

All four CO_{2Lag} smoothed data sets (Loess 2) identified in Table A10, Supplementary Material, Appendix A, were averaged to produce a composite CO_{2Lag} curve. Eight temperature data sets (Loess 2) also shown on Table A10, Supplementary Material, Appendix A, were averaged to produce a composite temperature curve. Both the CO_2 and temperature were taken from Data Set A. The four CO_{2Lag}, eight temperature, composite CO_{2Lag}, and composite temperature curves are all shown on Fig. 11. The CO_{2Lag} curves were corrected for CO_2 lag by 150 yr. Based on the temperature curves, warm periods and cool periods are shaded in light orange and light blue respectively. Key visually correlated peaks and troughs between CO_{2Lag} and temperature are shown in red and blue dashed lines respectively. Named warm and cool periods over the last 2000 yr are identified along the base of Fig. 11 after Easterbrook (2016a).

Fig. 11 unambiguously shows the close visual relationship of the composite curves of CO_{2Lag} (corrected for CO_2 lag by 150 yr) and composite temperature, as well as the non-lagged CO_2 curve, clearly out of phase with temperature. Conditional statistical correlation supports this observation with the following r_{PCC} data:

Year Range:	Data:	Correlation:	
1000 – 1600 AD	CO_{2Lag} (150-yr lag)	r_{PCC} = 0.93	Very Strong
1000 – 1600 AD	CO_2 (no lag)	r_{PCC} = 0.05	None
200 – 1600 AD	CO_{2Lag} (150-yr lag)	r_{PCC} = 0.73	Strong
200 – 1600 AD	CO_2 (no lag)	r_{PCC} = -0.07	None

The averaged pairs of CO_2 and temperature contain similar autocorrelation and long memory issues that its underlying component series have, and there may be additional artificial inflation of correlation due to smoothing and aggregation. However, of the 64 pairs of combinations from Table A10, Supplementary Material, Appendix A, 60 pairs have variants (Orig and/or RA 50) that have passed the SVF process as mostly Robustly Significant. In the averaged case four average CO_2 and temperature pairs (Orig, RA 50, RA 100, and Loess 2) have been tested with the SVF, and one pair successfully passed – the Orig pair. The results are shown in Table 3.

Table 3. Results of the SVF testing for the Average CO_2 vs. Average Temperature records Data Set A are shown for the range, 200-1600 AD. r_{PCC} is the Pearson's Correlation Coefficient; Samp Rate is the de-sampling rate to reduce the data points; n is the number of data points after de-sampling; Neff is the effective number of data points (Bretherton et al., 1999); Block-Perm-FDR p-values Grouped represents the process of using block permutations and grouped FDR (Fake Discovery Rate) showing p-values; HAC SE (Heteroskedasticity and Autocorrelation Consistent Standard Errors); and SVF Passing Category.

Results of Statistical Validation Framework Testing Average CO_2 vs. Average Temperature Correlation 200 -- 1600 AD								
Avg CO_2 & Temp Pair	r_{PCC}	Samp Rate	n	Neff	Block-Perm-FDR p-value Grouped	Blocks Passed	HAC SE	SVF Passing Category
CO_2 & Temp (Orig)	0.63	20	71	13.5	< 0.05	1,5,10	2.91	Robustly Significant
CO_2 & Temp (RA 50)	0.68	20	71	5.8	< 0.05	1,5	4.55	
CO_2 & Temp (RA 100)	0.71	30	47	4.7	< 0.05	1,5	4.89	
CO_2 & Temp (Loess 2)	0,72	20	71	2.7	< 0.05	1,5,10	32.8	

In Table 3 the Neff values on the Orig pair is strong, and the HAC SE value is commensurately low. Orig, RA 50, and RA 100, also passed on multiple blocks for FDR-grouped permutations p-value. The Neff values, being less than 8, are the primary reason for not passing SVF. Although Loess 2 for this averaged pair scenario is not directly validated under SVF, its correlation is presented here conditionally, supported by the corresponding Orig, passing Robustly Significant (SVF).

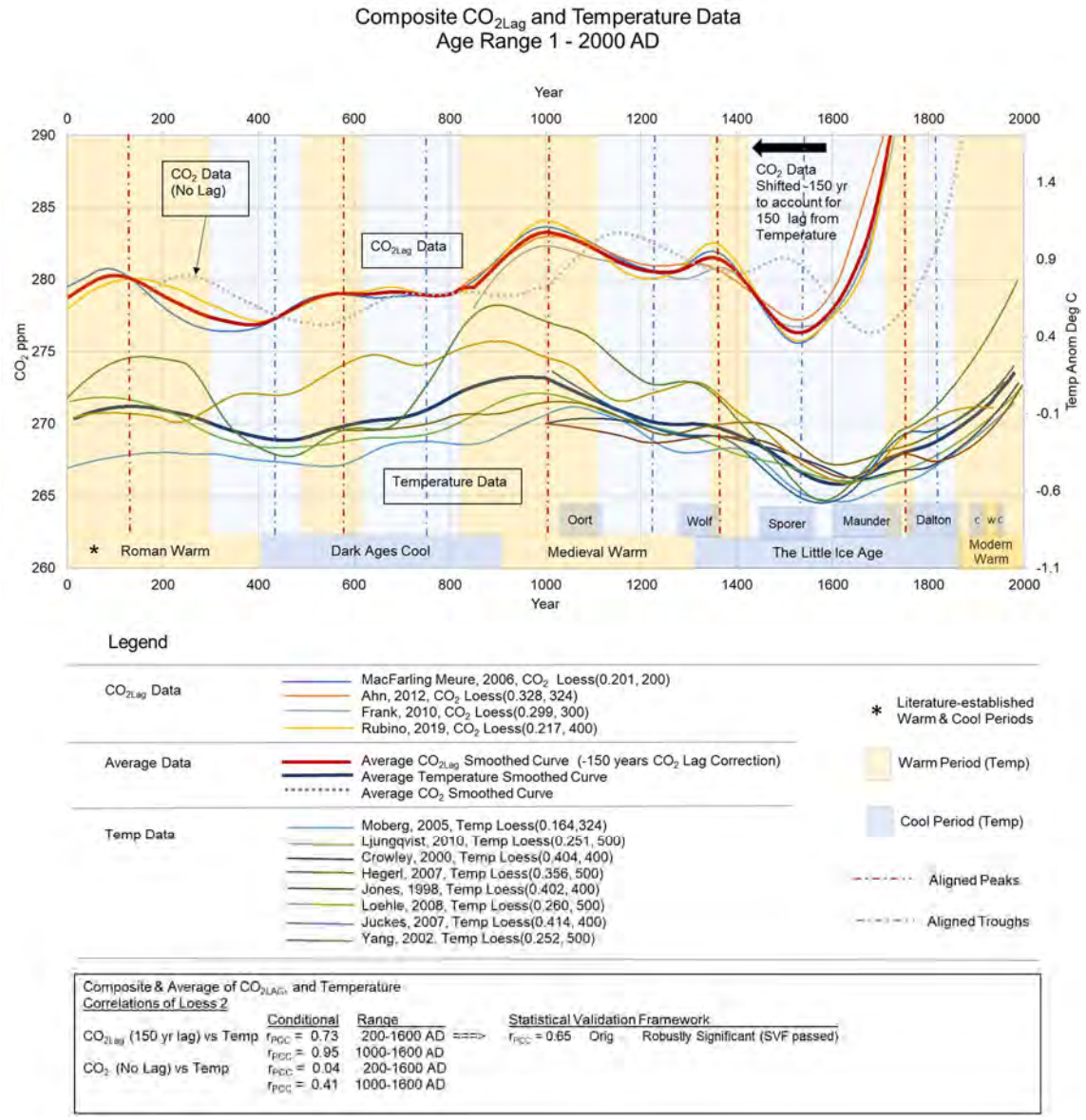

Figure 11. Smoothed Composite CO_{2Lag}, CO_2, and temperature data for the range of 1 to 2000 AD as well as average CO_{2Lag}, CO_2, and temperature. Cool and warm zones observed from this study are delineated as well as standard geologic-named cool and warm periods. Vertical red dashed lines identify visually correlated peaks between CO_{2Lag} and temperature. Vertical blue dashed lines identify visually correlated troughs between CO_{2Lag} and temperature. Averaged r_{PCC} values are shown for the lagged CO_2 and non-lagged CO_2 cases. Although Loess2 for this Average pair is not directly validated under SVF, its correlation is presented here conditionally, supported by the corresponding variant Orig, as Robustly Significant (SVF passed). High smoothing visually enhances apparent alignment, but should be statistically validated for formal inference. References: CO_2: Ahn et al. (2012), Frank et al. (2010), MacFarling Meure et al. (2006), and Rubino et al. (2019); Temperature: Moberg et al. (2005), Ljungqvist (2010), Crowley (2000), Hegerl et al. (2007), Jones et al. (1998), Loehle and McCulloch (2008), Juckes et al. (2007), Yang et al. (2002).

The average curves are shown without the composite curves for clarity on Fig. 12. The composite analysis confirms the individual analyses, both visually and statistically. Over the period of 1 to 1600 AD, CO_2 does not appear to control temperature in any manner. Rather, temperature appears to precede CO_2 in a closely coordinated process throughout the entire time period. This is shown by the visually coordinated curves of CO_{2Lag} and temperature after the CO_2 lag correction of 150 yr. The Very Strong r_{PCC} of 0.93 and 0.73 respectively for the two ranges analyzed, and the very low values of r_{PCC} for the non-lagged CO_2 data of $r_{PCC} = 0.05$ and $r_{PCC} = 0.07$ also contribute in this confirmation.

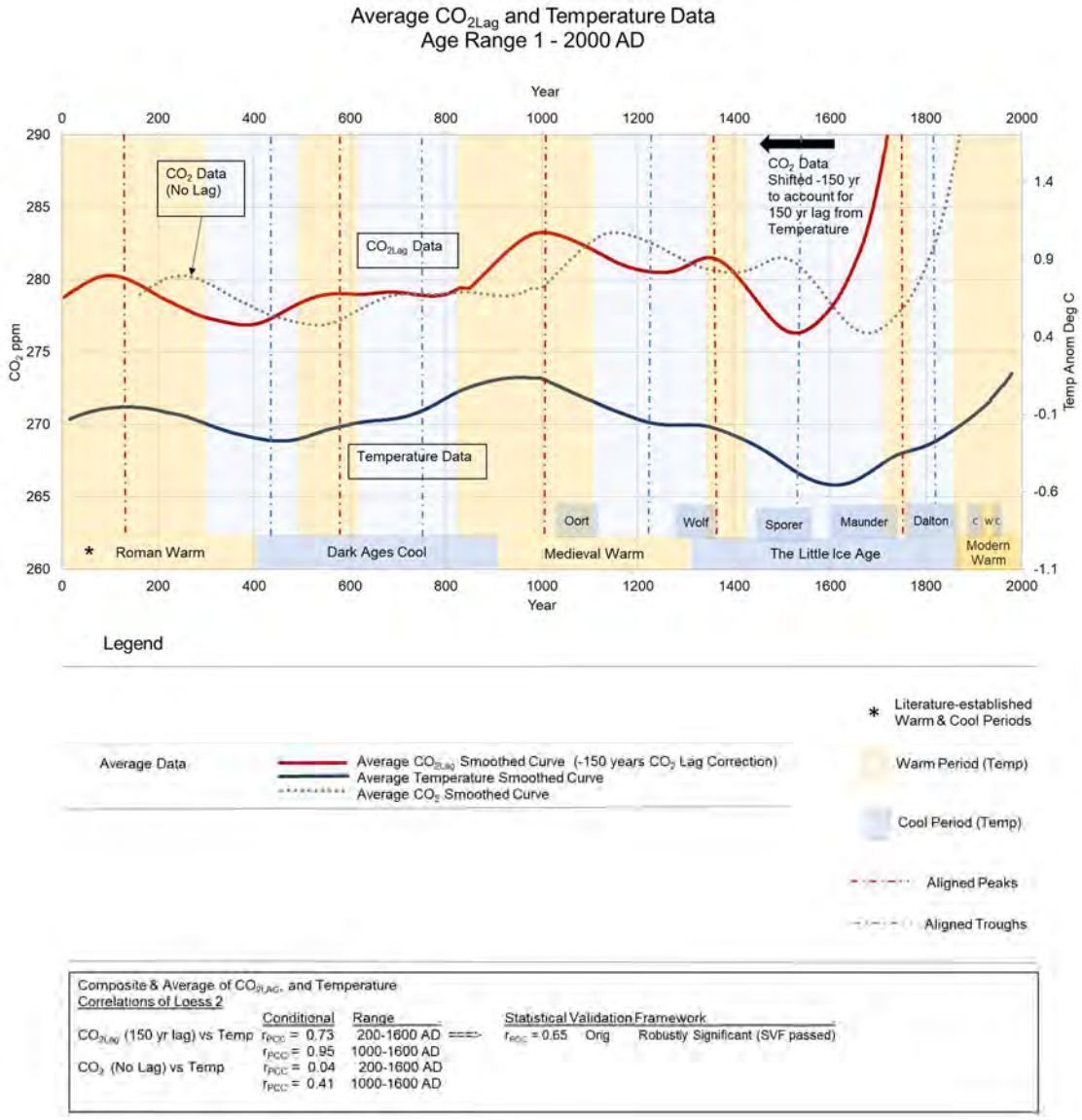

Figure 12. Smoothed Average CO_{2Lag}, CO_2, and temperature data for the range of 1 to 2000 AD. Cool and warm zones observed from this study are delineated as well as standard geologic-named cool and warm periods. Vertical red dashed lines identify visually correlated peaks between CO_{2Lag} and temperature. Vertical blue dashed lines identify visually correlated troughs between CO_{2Lag} and temperature. Averaged r_{PCC} values are shown for the lagged CO_2 and non-lagged CO_2 cases. Although Loess2 for this Average pair is not directly validated under SVF, its correlation is presented here conditionally, supported by the corresponding variant Orig, as Robustly Significant (SVF passed). High smoothing visually enhances apparent alignment, but should be statistically validated for formal inference. References: CO_2: Ahn et al. (2012), Frank et al. (2010), MacFarling Meure et al. (2006), and Rubino et al. (2019); Temperature: Moberg et al. (2005), Ljungqvist (2010), Crowley (2000), Hegerl et al. (2007), Jones et al. (1998), Loehle and McCulloch (2008), Juckes et al. (2007), Yang et al. (2002).

3.8 Graphical Results – Smoothed CO_2 and Temperature (1600-1850 AD)

As discussed in Section 3.3 and detailed further in Supplementary Material, Appendix C, a structural break, consistent with a broader regime shift in climate dynamics, was identified around 1600 AD. This apparent state transition introduces a discontinuity in the statistical behavior of the system, particularly in the correlation between atmospheric CO_2 and temperature. For example, Pearson's correlation coefficients (r_{PCC}) are internally consistent within each period (e.g., 200–1600 AD and 1600–1850 AD), and even generally consistent between the two periods, but they degrade significantly when calculated across the boundary. Periods that span this breakpoint—such as 200–1650 AD or 200–1850 AD—show a marked decline in correlation strength, transitioning from strong to weak or nonsignificant values. To account for this discontinuity, the present study analyzes the two time periods separately:

1. a pre-break interval from 200–1600 AD, and
2. a post-break interval from 1600–1850 AD.

The upper bound of 1850 AD was selected based on the availability of robust correlation between CO_2 and temperature after applying a 150-yr lag correction to the CO_2 data—consistent with lag patterns observed throughout this study. Beyond 1850 (i.e., post-2000 when adjusted for lag), no valid comparisons can be drawn due to the absence of viable lag-corrected CO_2 data. This section presents the graphical and statistical analyses of the 1600–1850 AD interval, highlighting key patterns in the CO_2–temperature relationship during this climatically transitional period.

This section of the study investigates the conditional statistical association and visual graphical correlation between atmospheric CO_2 concentrations and multiple paleotemperature proxies over the period 1600-1850 AD by employing Running Average (RA 50) smoothing with a 50-yr centered window on all series. Three independent CO_2 records—Ahn et al. (2012), MacFarling Meure et al. (2006), and Rubino et al. (2019)—are analyzed against six established temperature reconstructions. Data results are shown in Supplementary Material, Appendix A, Table A23. Key findings are summarized below (average r_{PCC} of each temperature vs. the three CO_2 series):

Temperature	Average r_{PCC} No Lag	Average r_{PCC} Lag Max	Average Lag Years
Crowley (2000)	0.25	0.90	170
Hegerl (2007)	0.46	0.96	183
Juckes (2007)	0.43	0.99	223
Ljungqvist (2010)	0.68	0.90	203
Moberg (2005)	0.63	0.90	163
Yang (2002)	0.46	0.92	193
Overall Averages	0.45	0.90	189

Significant points:

1. There is a significant increase between the No Lag and Lagged r_{PCC} values – the average correlation is 2 times higher for lagged vs. no lagged scenarios. This is similar to the data from the data range 200-1600 AD.
2. The max r_{PCC} values (0.90- 0.99) and the no lag r_{PCC} (0.25 – 0.68) values are both within the close range of the r_{PCC} values in the data range 200-1600 AD, albeit slightly higher.

As with other data in this study, the 1600-1850 AD data have been processed through the SVF to better understand the significance of the correlations. Table 4 depicts the results of the SVF. There is one CO_2 and temperature pair that passed the SVF in either of the two passing categories. Rubino CO_2 (Orig) vs. Moberg Temp (Orig) passed as Robustly Significant with a Neff value over 10 and group-block-permutation-FDR p-value < 0.05 in at least one block. It also had an r_{PCC} = 0.54, sample size of 10, and HAC SE = 150.97. The HAC SE values were higher overall than the data from range 200-1600 AD possibly due to the regime change at 1600 AD and the exponentially increasing rates of increase for the CO_2 and temperature data commencing in this

timeframe. Five of the pairs exhibited Neff between 5 and 7; passed the p-value test of Grouped-Block-Perm-FDR with values < 0.05; and all had reasonable strong sample sizes with r_{PCC} between 0.52 and 0.80 (4 Orig and 1 RA 100). While these five pairs did not pass the stringent SVF, they exhibited strong parameters. The last three pairs are noteworthy from the perspective they had strong enough Neff values, but faltered in the Grouped-Block-Perm-FDR, which indicates strong Neff values alone are not enough.

As mentioned above, the goal of the SVF is not to suppress correlation results but to distinguish robust signal from statistical artifact in the presence of serial correlation and long-term memory issues. The results from 1600-1850 AD are consistent with those of 200-1600 AD, although there is a much lower pass rate probably related to regime change and rapid rise in CO_2 and temperature commencing in this time period. Along with the visual correlations shown below, the data does conditionally indicate some marginal significance (Santer et al., 2000; von Storch & Zwiers, 1999; Bretherton et al., 1999).

Table 4. Results of the SVF testing for the CO_2 vs. temperature records from Data Set A are shown for the range, 1600-1850 AD . r_{PCC} is the Pearson's Correlation Coefficient; Samp Rate is the de-sampling rate to reduce the data points; n is the number of data points after de-sampling; Neff is the effective number of data points (Bretherton et al., 1999); Grouped-Block-Perm-FDR p-values represents the process of using block permutations and grouped FDR (Fake Discovery Rate) showing p-values; HAC SE (Heteroskedasticity and Autocorrelation Consistent Standard Errors); and SVF Passing Category.

Results of Statistical Validation Framework Testing CO_2 vs. Temperature Correlations 1600 -- 1850 AD								
Avg CO_2 & Temp Pair	r_{PCC}	Samp Rate	n	Neff	Grp-Block-Perm-FDR p-value	Blocks Passed	HAC SE	SVF Passing Category
Rubino CO_2 (Orig) Moberg Temp (Orig)	0.54	10	22	12.31	< 0.05	1	150.97	Robustly Significant
Ahn CO_2 (Orig) Hegerl Temp (Orig)	0.84	10	16	6.18	< 0.05	1	7.68	-
MacFarling CO_2 (Orig) Hegerl Temp (Orig)	0.52	10	23	5.51	< 0.05	1	152.85	-
Ahn CO_2 (RA 100) Moberg Temp (RA 100)	0.80	10	11	5.51	< 0.05	1	41.17	-
Rubino CO_2 (Orig) Hegerl Temp (Orig)	0.71	10	22	5.32	< 0.05	1	10.28	-
Rubino CO_2 (Orig) Crowley Temp (Orig)	0.64	10	22	5.00	< 0.05	1	34.61	-
Ahn CO_2 (Orig) Moberg Temp (Orig)	0.18	10	16	14.02	> 0.05	-	74.22	-
MacFarling CO_2 (Orig) Moberg Temp (Orig)	0.39	10	23	13.16	> 0.05	-	49.55	-
MacFarling CO_2 (Orig) Crowley Temp (Orig)	0.35	30	8	8.18	> 0.05	-	21.47	-

Figure 13 presents the transformed CO_2 and temperature series from Ahn et al. (2012) and Hegerl et al. (2007), respectively, for the period 1600–1850 AD as RA 50. The CO_2 series was cubed, detrended with linear regression, and normalized to a common scale from 0.0 to 1.0, and the x-

axis extends from 1600 to 2000 AD to display the full temporal extent of the data, including lag alignment. The temperature series was normalized to match the CO_2 data. The purpose of this display style is due to the exponentially rising CO_2 and temperature curves. The transformation mollifies the chart without changing relationships to allow more character to be observed. The lag-adjusted CO_2 series (CO_{2Lag}, red), the unadjusted CO_2 series (gray dashed line), and the temperature series (blue) are plotted, with the CO_{2Lag} offset by 170 yr. Vertical reference lines mark visually striking coincident peaks and troughs between CO_{2Lag} and temperature, which are now visible due to the transformations. This alignment is quantitatively supported by a conditional Pearson correlation coefficient (r_{PCC}) of 0.95, compared to a much weaker correlation of 0.48 between the non-lagged CO_2 and temperature series. RA 50 for this pair is not directly validated under SVF, nor is its Orig variant. Its correlation is presented here conditionally, supported by SVF showing marginal significance with marginal Neff and passing FDR, and a related pair, Rubino CO_2 (Orig) and Moberg Temp (Orig), showing the corresponding variant, Orig, Robustly Significant (SVF passed). High smoothing visually enhances apparent alignment, but should be statistically validated for formal inference.

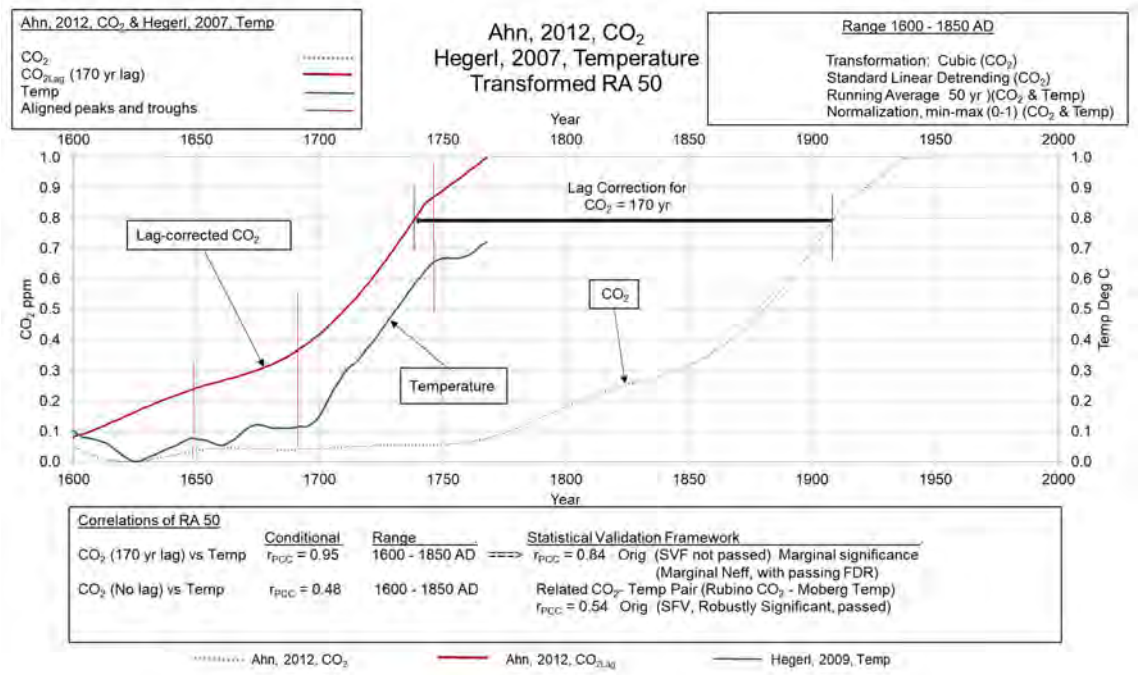

Figure 13. Running Average, RA 50 smoothing, CO_2 and temperature data (from Ahn et al., 2012; Hegerl, 2007, respectively), are shown from 1600 to 2000 AD along with the CO_2 curve shown with a 170-yr lag correction. CO_2 is cubed, detrended with a linear regression, and normalized.between 0-1. Temperature is normalized between 0-1. Aligned peaks and troughs are depicted with thin red lines. Conditional maximum r_{PCC} correlations at lag and r_{PCC} at no lag are presented. Although RA 50 for this pair is not directly validated under SVF, nor is its Orig variant, its correlation is presented here conditionally, supported by SVF showing marginal significance with marginal Neff and passing FDR, and a related pair, Rubino CO_2 (Orig) and Moberg Temp (Orig), showing the corresponding variant, Orig, Robustly Significant (SVF passed). High smoothing visually enhances apparent alignment, but should be statistically validated for formal inference.

Figure 14 displays a very similar chart to Figure 13. The transformed CO_2 and temperature series from Rubino et al. (2019) and Hegerl et al. (2007), respectively, for the period 1600–1850 AD. The CO_2 series was cubed, detrended with linear regression, and normalized to a common scale from 0.0 to 1.0, and the x-axis extends from 1600 to 2000 AD to display the full temporal extent of the data, including lag alignment. The temperature series was normalized from 0-1. The lag-adjusted CO_2 series (CO_{2Lag}, red), the unadjusted CO_2 series (gray dashed line), and the temperature series (blue) are plotted, with the CO_{2Lag} off-set by 180 yr. Vertical reference lines mark visually striking coincident peaks and troughs between CO_{2lag} and temperature, which are now

visible due to the transformations. This alignment is quantitatively supported by a conditional Pearson correlation coefficient (r_{PCC}) of 0.97, compared to a weaker correlation of 0.43 between the non-lagged CO_2 and temperature series. Although RA 50 for this pair is not directly validated under SVF, nor is its Orig variant, its correlation is presented here conditionally, supported by SVF showing marginal significance with marginal Neff and passing FDR, and a related pair, Rubino CO_2 (Orig) and Moberg Temp (Orig), showing the corresponding variant, Orig, Robustly Significant (SVF passed). High smoothing visually enhances apparent alignment, but should be statistically validated for formal inference.

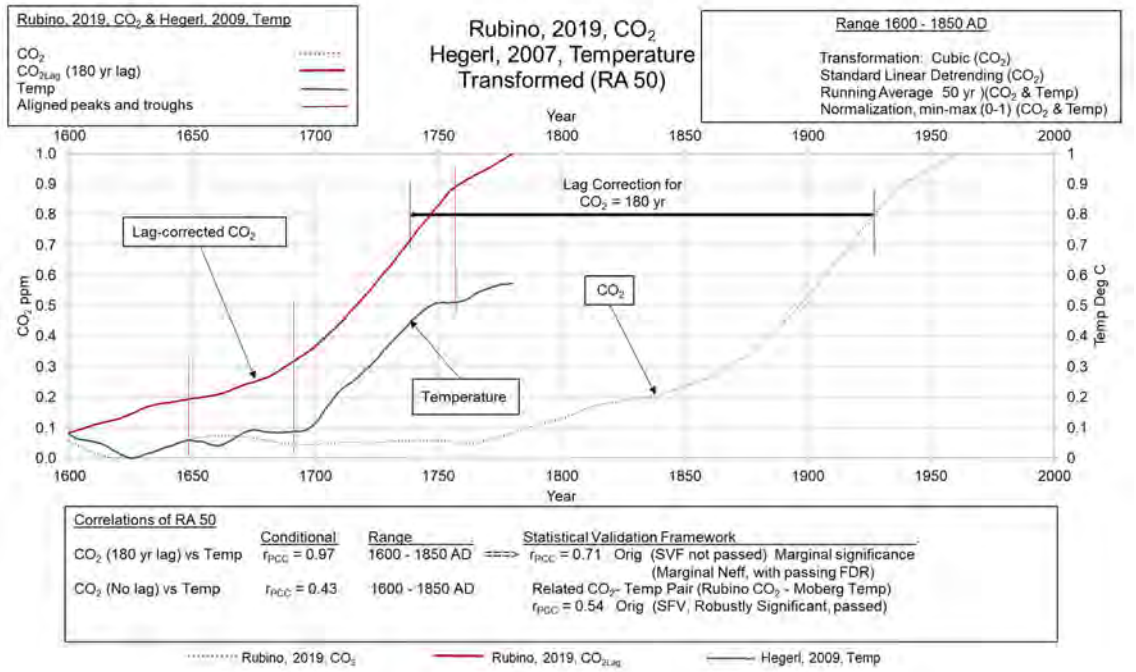

Figure 14. Running Average, RA 50 smoothing, CO_2 and temperature data (from Rubino et al., 2019; Hegerl, 2007, respectively), are shown from 1600 to 2000 AD along with the CO_2 curve shown with a 180-yr lag correction. Aligned peaks and troughs are depicted with thin red lines. Conditional maximum r_{PCC} correlations at lag and r_{PCC} at no lag are presented. Although RA 50 for this pair is not directly validated under SVF, nor is its Orig variant, its correlation is presented here conditionally, supported by SVF showing marginal signifi-cance with marginal Neff and passing FDR, and a related pair, Rubino CO_2 (Orig) and Moberg Temp (Orig), showing the corresponding variant, Orig, Robustly Significant (SVF passed). High smoothing visually enhances apparent alignment, but should be statistically validated for formal inference.

Fig. 15 displays the Pearson Correlation Coefficient, r_{PCC}, plotted against a range of CO_2 lag values (-100 to 250). The curve in this example shows a flat peak area ranging between r_{PCC} of 0.90 and 0.92 between lags of 160 to 195 yr. r_{PCC} drops off quickly in either direction before and after the flat peak.

These figures highlight the very strong relationship between lag-adjusted CO_2 and temperature, and reinforces a critical observation: once CO_2 is corrected for its lag (~170 to 180 yr), little comparable data remain in the late 20th and early 21st centuries to inform centennial or millennial-scale analyses. Notably, the more granular analyses by Koutsoyiannis (2024a), Humlum et al. (2013), Chylek et al. (2018b), and Adams and Piovesan (2005) report that CO_2 lags temperature by less than one year during the modern instrumental era. These studies typically assess monthly or annual fluctuations over relatively short time spans and likely capture dynamics distinct from those observed at centennial or millennial scales.

Therefore, the lag observed in the present study from 200-1600 AD and 1600-1850 AD (~150–170 yr) does not contradict the findings of these short-term studies. Rather, the consistent and strong correlation between CO_{2lag} and temperature throughout the last 2000 yr—using annual

resolution data—suggests a robust long-term relationship where temperature changes consistently precede CO_2 over centennial timescales.

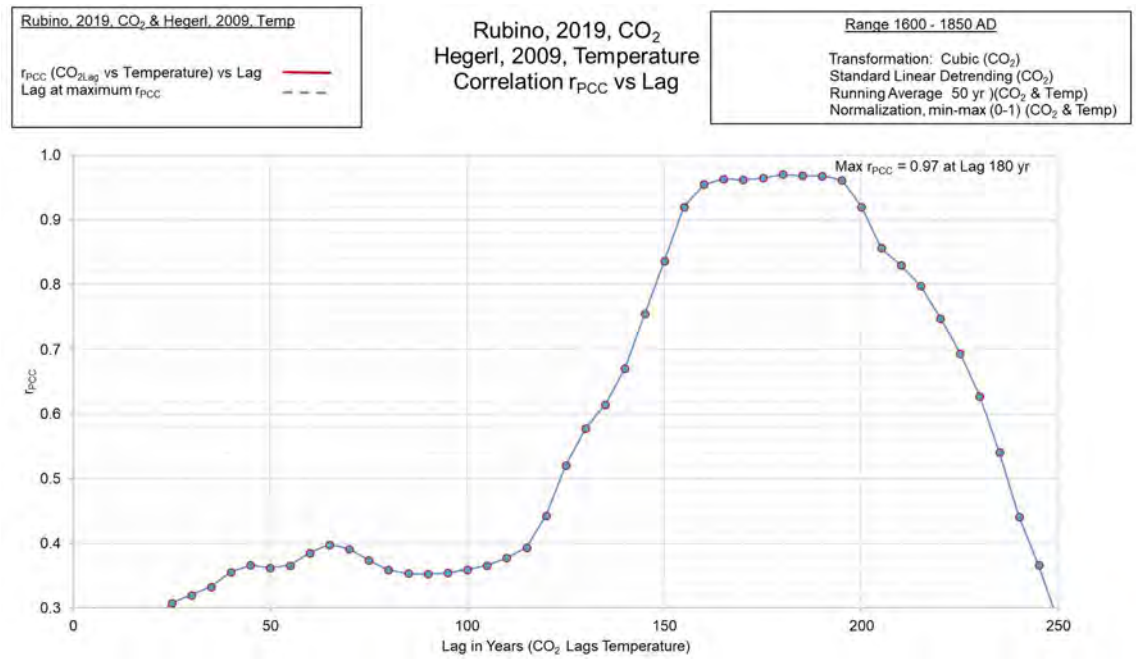

Figure 15. Pearson Correlation Coefficient, r_{PCC}, is plotted against CO_2 lag corrections (-100 to 250, interval of 5 yr) for CO_2 (Rubino et al., 2019) and temperature (Hegerl et al., 2007). The peak of the curve depicting maximum correlation is at 180 yr of CO_2 lag correction. Correlation drops off in either direction rapidly after the flat peak area.

3.9 Total Solar Irradiance (TSI) and Temperature (1-2000 AD)

A comparative analysis was performed between multiple published reconstructions of Total Solar Irradiance (TSI) and temperature data spanning the past two millennia as detailed in Supplementary Material, Appendix D. Using conditional Pearson correlation coefficients with input on significance from the SVF, both visual and statistical congruence were identified across a broad array of TSI reconstructions (e.g., Scafetta & Bianchini, 2022; Scafetta, 2023; Lean, 2018; Shapiro et al., 2011; Wu et al., 2018; Steinhilber et al., 2009) and temperature datasets (e.g., Ljungqvist, 2010; Morice et al., 2012 [HadCRUT4]; Lenssen et al., 2024 [GISS]; Parker et al., 1992 [CET]). Similar to the previous conditional analysis of CO_2 and temperature, this analysis accounts for autocorrelation and long-term memory in paleoclimatic records. Given this caveat, Strong to Very Strong correlations were observed between TSI and global atmospheric temperature, reinforcing the hypothesis that TSI variability represents solar energy, which has been a persistent contributor to centennial-scale temperature dynamics. Integrating the TSI–temperature analysis alongside the CO_2–temperature analysis provides a more comprehensive perspective on the potential dynamic relationships among solar energy, surface temperature, and atmospheric CO_2.

4. Discussion

4.1 Atmospheric CO_2 Lags Temperature by 150 yr

Results from both original and smoothed datasets—derived from visual inspection and correlation analysis—indicate that global atmospheric CO_2 lags atmospheric temperature by approximately 150 years over the period 1–1850 AD. Although the Industrial Revolution began around 1750 AD (Wilson, 2014), significant anthropogenic CO_2 emissions did not occur until roughly 1930 AD (Hoesly, 2018). This finding suggests that the observed lag is a natural process, as is the

subsequent exponential increase in CO_{2Lag} from ~1600 AD to the present in response to rising temperatures.

Because this analysis shows that CO_2 change has continuously followed temperature change throughout the Common Era—including 1850–2000 AD CO_2 changes that reflect temperature changes from 1700–1850—there is no evidence for a fundamental change in the CO_2–temperature relationship over the last 150 years.

Figures 11 and 12 summarize the smoothed CO_{2Lag} and temperature curves, which visually track each other closely from 1–1600 AD. Figures 13 and 14 show a similar close correspondence from 1600–1775 AD. In all four figures, vertical dashed lines (red for peaks, blue for troughs) mark the synchronous occurrence of every identified peak and trough in CO_{2Lag} and temperature over nearly 1800 years.

The combined evidence indicates that CO_2 does not exert a primary control on Earth's temperature over this time period; rather, it closely tracks temperature with a lag of ~150 yr. The analysis also reveals a structural break or regime shift around 1600 AD, coinciding with both the nadir of the Little Ice Age (Maunder Minimum) and a solar energy minimum, which corresponds to the observed temperature low and subsequent rapid increase in both temperature and lag-corrected CO_2. Between 1600 and 1850, the visual and statistical correlations between CO_{2Lag} and temperature are strong.

The original CO_2 and temperature curves (Figs. 1–2), along with RA 50 (Fig. 4) and RA 100 (Fig. 5) series, strongly agree with the Loess smoothed-curve analyses (Figs. 6–10). All original datasets exhibit a pronounced concurrent drop in temperature and CO_{2Lag} around 1460 AD, with a narrow 50–80 yr width. This distinct feature is only apparent after applying the −150 yr CO_2 lag correction and is further supported by:

1. Long-term patterns: The data suggest a possible millennial-scale cycle, with peaks near 100, 1000, and 2000 AD, and troughs around 550 and 1450 AD (~1000 yr frequency). Both CO_{2Lag} and temperature appear to track this pattern, which aligns with proposed solar activity cycles such as the Eddy Cycle (Abreu et al., 2010; Zhao et al., 2020) and Hallstatt Cycle (Steinhilber et al., 2010). Longer datasets would be required to confirm a true cycle.
2. Shorter-term variability: Numerous visually correlated peaks, troughs, and peak–trough clusters are evident throughout 1–1850 AD, on timescales of 10–100 yr.

This mirrored relationship between CO_{2Lag} and temperature appears at multiple temporal scales:

1. Macro-scale (~2000 yr): millennial cycles
2. Meso-scale (10–100 yr): decadal–centennial variability
3. Micro-scale (months): as documented by other studies

For example, Humlum et al. (2013) found that monthly CO_2 lags global SST by 11–12 mo and global air temperature by 9.5–10 mo (1980–2011 instrumental data). Monnin et al. (2001) identified a ~410 yr CO_2 lag during 11.2–17.0 kyr BP. Sharma and Karamanev (2021) reported a 1020–1080 yr lag over the last 650 kyr (max $r_{PCC} = 0.837$). Koutsoyiannis (2024a) demonstrated varying CO_2–temperature lags at multiple geologic periods, from 2.3 Myr in the Phanerozoic to 3–8 mo in the modern instrumental era.

Collectively, these findings, combined with the ~150 yr lag identified here, suggest that different but related processes drive the CO_2–temperature lag at different timescales. Humlum et al. (2013) proposed that near-surface ocean temperatures are a primary cause for short-term lags. The millennial-scale lag found by Sharma and Karamanev (2021) may reflect deeper ocean processes. Adams and Piovesan (2005) further proposed that monthly lags may involve internal biogeochemical cycles and tropical temperature influences.

4.2 Statistical Validation Framework

The inclusion of r_{PCC} analysis in concert with the visual correlation of CO_{2Lag} (150 yr) and

temperature and the visual correlation of TSI and temperature is based on a robust correlation testing framework, Statistical Validation Framework (SVF). It is implemented to assess statistical reliability of observed correlations between lag-adjusted atmospheric CO_2 proxies and temperature reconstructions as well as Total Solar Irradiance (TSI) and temperature. The analysis incorporates block permutation testing (10,000 iterations) across multiple block sizes, HAC-consistent standard errors, and both global and grouped FDR corrections to rigorously control for autocorrelation and long memory. Passing pairs were filtered based on effective sample size (Neff), yielding results classified as Robustly Significant (Neff ≥ 10) or Tentatively Significant (Neff 8–10), providing a conservative assessment of correlation reliability across time series with complex temporal structure. The SVF has successfully identified key correlation pairs that show significance through the camouflage of dependence, serial correlation, and long memory.

4.3 Role of the Oceans in the Relationship of CO_2 to Temperature

Humlum et al. (2013) states that changes in ocean temperatures appear to explain most of the changes in atmospheric CO_2 during the 1980 to 2011 period, especially changes in Southern Ocean temperature.

Ocean processes and the carbon cycle are potential areas to investigate the possible explanations for the lag of CO_2 to temperature, especially deep ocean carbon sinks (Wang et al., 2024), atmospheric CO_2 ventilation (Yu et al., 2023), and the global ocean conveyor circulation (Toggweiler & Key, 2001). For the 150-yr CO_2 lag identified in this study, the answer may be related to deeper ocean processes as well as biogeochemical processes. It has been established by many researchers that CO_2, as part of the carbon cycle, is absorbed in the ocean as a carbon sink, when the temperature of the water is cool, and conversely, CO_2 is released into the atmosphere when the temperature of the water is warm (Easterbrook, 2016b), but the process is more complex as noted by (Wang et al., 2024), (Yu et al., 2023), and (Toggweiler & Key, 2001). Additional investigation is required to establish the process causing CO_2 to lag temperature, but the facts, as outlined in this study and the studies (Adams & Piovesan, 2005; Chylek et al., 2018b; Humlum et al., 2013; Monnin et al., 2001, Caillon et al., 2003; Mudelsee, 2001; Koutsoyiannis, 2024a; and Sharma & Karamanev, 2021), identify that CO_2 lags temperature at all major timeframes: months, tens of years, hundreds of years, hundred thousands of years, and even millions of years. These studies, as well as this study, also identify that CO_2 does not influence temperature.

4.4 Total Solar Energy (TSI) correlates with Temperature

This study and others have established that atmospheric CO_2 lags both atmospheric and sea surface temperature. The next important question is the source of influence on the temperature of the oceans and atmosphere. Accordingly, this study has evaluated the data from several TSI papers and compared these with temperature data assessed in this study. The time period covers the last 2000 yr and the last few hundred years respectively.

Fig. D1, in Supplementary Material, Appendix D, defines a very close correlation between temperature (Ljungqvist, 2010) and TSI (Shapiro et al., 2011) as evidenced by the tight visual tracking and Very Strong conditional statistical correlation ($r_{PCC} = 0.79$ for the range of 5 to 1994 AD; $r_{PCC} = 0.91$ for the range of 1000 to 1994 AD). Causation cannot be proven from a chart such as this, but it is difficult to imagine how solar energy does not play a major role in control of atmospheric temperature from consistent results that span 2000 yr. It is probably a matter of determining the characteristics of the solar energy which is the major influencer. Fig. D2, in Supplementary Material, Appendix D, utilizing three different TSI studies (Steinhilber et al., 2010; Lean, 2018; Wu et al., 2018) shows TSI versus the Average Temperature curve (Fig. 12) taken from averaging temperature from eight temperature studies. While the visual correlation is quite compelling, and the correlation analysis is Strong ($r_{PCC} = 0.61$ to 0.62 for the range of 5 to 1994 AD; $r_{PCC} = 0.65$ to 0.75 for the range of 1000 to 1994 AD), the differences in Fig. D2, in Supplementary Material, Appendix D, compared to Fig. D1, in Supplementary Material, Appendix D, identify a slightly greater variability and less precision.

Switching the timeframe to the 250-yr range, Fig. 19 depicts TSI data from Scafetta (2023) compared to three temperature data sets collected instrumentally. These data are maintained by the Met Office Hadley Centre in Great Britain and are smoothed using Loess in this study: (1) HadCRUT4 (atmospheric temperature) (Morice et al., 2012), (2) HadSST3 (sea surface temperature) (Kennedy et al., 2011a; Kennedy et al., 2011b), and (3) CET (Legacy version) (atmospheric temperature of central England) (Parler et al., 1992). These data present as highly visually correlated on the chart and have a Very Strong statistical correlation ranging from $r_{PCC} = 0.84$ to $r_{PCC} = 0.92$. Thus, it appears the same results are evident regarding the close correlation of TSI and temperature both at very short and granular timeframes of 200 yr to longer periods of 2000 yr.

In Fig. D4, in Supplementary Material, Appendix D, all three temperature curves appear to trend sharply upward from about 1995 through 2023, whereas the TSI curve makes a significant lower turn. This appears to be somewhat discordant with the rest of the entire curve comparison from 1800 to present. One possible explanation has been proffered by several researchers as an artifact of five factors, especially for the years since 1995, which are:

1. Urban Heat Effect – a well-known result of temperature measurement stations being located in cities, airports, and urban areas exhibiting a significant increase of temperature over the ambient baselines as much as 0.45 degrees C. (Scafetta, 2021; Soon et al., 2023; Katata et al., 2023; Spencer, 2024; Watts, 2012)
2. Multiple questionable data adjustments since 2000 AD by organizations responsible for temperature repositories, such as NOAA, NASA, and Met Office Hadley Centre. The adjustments have typically increased parts of the temperature record by as much as 0.2 to 0.4 degrees C. (McKitrick, 2010; US Historical Climatological Network, 2024; Watts, 2012; Wallace et al., 2017)
3. Reduction of temperature stations by as much as 25% or more in mostly rural areas and a practice of populating the removed stations data with calculated estimates. (McKitrick, 2010; Wallace et al., 2017)
4. Natural temperature-enhanced forcing from large El Nino events (Douglass & Christy, 2009; Vinos, 2024b; Cobb et al., 2003)
5. An underwater volcanic eruption in 2022, Tonga, which increased water vapor in the global atmosphere by 10%, causing a sharp increase in global temperature, which will take several years to dissipate (Bielfeld, 2023; Vinos, 2024a; Vinos, 2024b; Lee & Wang, 2022).

The significant steep trough of TSI at about 1460 yr AD shown in Fig. 20 for all 4 TSI studies at a slight smoothing, is also replicated on all of the temperature and CO_{2Lag} data sets shown in Fig. 1, Fig. 2, Fig. 4, and Fig. D5, in Supplementary Material, Appendix D. This marker, at 1460 AD, coupled with the overall visual and statistical correlations of these data, emphasize the relationship of these data to each other.

A strong correlation of TSI and atmospheric global temperature over a 2000-yr period is probably not a coincidence. Solar energy either plays an integral part in controlling temperature on the earth, or another forcing agent influences both solar energy and temperature. Perhaps, a third option is possible, where solar energy plays a major role in controlling temperature in concert with other agents (Scafetta, 2023). Some of these agents could include ocean and atmospheric pressure processes (D'Aleo & Easterbrook, 2016) such as the Atlantic Multidecadal Oscillation (AMO) (Knudsen et al., 2011), El Nino Southern Oscillation (ENSO) (Trenberth, 2016), or Thermohaline Ocean Circulation (THC) (Toggweiler & Key, 2001), among others (D'Aleo & Easterbrook, 2016). Cloudiness appears to be a significant contributor as well, as it appears to be controlled by solar magnetic modulation of cosmic rays (Svensmark et al., 2021; Svensmark et al., 2016; Svensmark, 2007). Volcanism also seems to correlate with temperature decreases as shown over the Little Ice Age (1250-1860 AD) (Wanner et al., 2022). On a larger scale, orbitally-driven insolation forcing, mainly precession and obliquity, can have influence (Wanner et al., 2022; Lorenz et al., 2006). Another indirect impact of TSI is solar-driven weakening of the jet stream causing colder temperatures in the northern hemisphere (Schwander et al. 2017; Moffa-Sanchez

et al., 2014; Ineson et al., 2011). However, based on the strong visual and statistical correlations between TSI and temperature over short, medium, and longer time periods (2000 yr) shown in this study, it appears that solar energy is most probably a significant component, either directly or indirectly, in concert with other natural processes previously mentioned, controlling the temperature of the earth.

5. Conclusions

Atmospheric CO_2 clearly lags global temperature by about 150 yr over the timeframe of 1 to 1850 AD as shown by both visual and conditional statistical correlations (Very Strong) using all 16 atmospheric temperature studies compared with all 4 CO_2 studies for both original data and smoothed data.

Total Solar Irradiance (TSI) correlates both visually and statistically (conditional) with the data from the large number of temperature studies utilized in this paper:

1. Six TSI data sets compared to temperature from Ljungqvist (2010) and the Average Temperature from 8 atmospheric temperature studies over the last 2000 yr (Strong r_{PCC}).
2. Two additional TSI data sets compared to five shorter-term temperature data sets in the timeframe of 1850 to present (Very Strong r_{PCC}).

Along with many other correlated data curve artifacts such as peaks and troughs, a striking downward dip at the year, 1460 AD, is observed on all related data:

1. Atmospheric temperature
2. CO_{2Lag} of 150 yr
3. Total Solar Irradiance

The Statistical Validation Framework (SFV) supported the conditional use of the r_{PCC} values for comparative purposes based on a robust testing process taking into account dependence, autocorrelation, and long-term memory issues.

Atmospheric CO_2 does not precede temperature, nor does it control temperature as shown in this study over the last 2000 yr. The same conclusions have been reached in the study by Koutsoyiannis (2024a) coving several geologic time periods (e.g. Modern Period, Common Era, and Phanerozoic) over varying degree of CO_2 lag.; Humlum et al. (2013) for the monthly timeframe in the time period of 1980 to 2010, for 9 to 12 mo; Chylek et al. (2018b) between 1960 and 2016 for monthly data for 5 mo; and Adams and Piovesan (2005) between 1960 and 2004 for monthly data for 4 mo. The study by Sharma and Karamanev (2021) reached the conclusion CO_2 lags temperature by over 1000 yr over the last 650,000 yr.

It appears temperature, especially ocean temperature, plays a major and significant role in the consistent change of atmospheric CO_2, either directly or indirectly, with other oceanic processes. TSI correlates strongly with atmospheric temperature over the last 2000 yr (r_{PCC} is Strong) and over the shorter period of the last 200 yr (r_{PCC} is Very Strong) lending more evidence that solar energy plays a significant role in the temperature change of the earth.

Thus, a likely scenario for earth's climate change is driven by solar energy controlling temperature, directly or indirectly, and temperature controlling CO_2 somewhat modified by other climate factors. As such, this progression is likely influenced to some degree by several other wide-ranging processes from disparate sources such as: orbital-driven insolation forcing; vulcanism; change in cloudiness due to solar magnetic modulation of cosmic rays; planetary gravity; earth global and orbital mechanics; solar sub-processes; ocean circulation, oscillations, and cycles; atmospheric pressures; polar vortexes; solar-driven weakening of the jet stream; and others.

Acknowledgements

This study could not have been accomplished without access to published data and international databases on temperature, atmospheric CO_2, and total solar irradiance. I am grateful to Dr. Ole Humlum for encouragement and informal discussion on this topic as well as peer reviewer, Professor Demetris Koutsoyiannis for structured, critical, and constructive evaluation which has hopefully led to more clarity, accuracy, focus, and scientific merit.

Supplementary Material

Supplementary Material for this article includes Appendices A–D: (A) Data – Correlation Analysis of CO_2 vs. temperature, (B) Statistical Validation Framework, (C) Structural Break or Regime Shift at 1600 AD, and (D) Total Solar Irradiance and Temperature. It is available at Science of Climate Change online:
https://scienceofclimatechange.org/wp-content/uploads/SM-Vol5.3-Grabyan.pdf

Declarations

This research did not receive any specific grant from funding agencies in the public, commercial, or not-for-profit sectors. The author declares that there are no known competing financial interests or personal relationships that could have appeared to influence the work reported in this paper.

Editor: H. Harde; **Reviewers**: D. Koutsoyiannis and anonymous.

References

Abdussamatov, H., 2015. *Current Long-term Negative Average Annual Energy Balance of the Earth Leads to the New Little Ice Age*. Thermal Science, 19. S279-S288.

Abdussamatov, H., 2016. *The began quasi-centennial epoch of the New Little Ice Age*. In Abstract Book, Eleventh Annual Conference, "Plasma Physics in the Solar System", February 15-19, 2016. Space Institute of the RAS, Moscow, p 187 (in Russian). https://doi.org/10.1016/B978-0-12-804588-6.00017-3.

Abreu, J. A., Beer, J., Ferriz-Mas, A., 2010. *Past and Future Solar Activity from Cosmogenic Radionuclides*. In Cranmer, S. R., Hoeksema, T. Kohl, J. L. (Ed.), 2010. SOHO-23: Understanding a Peculiar Solar Minimum ASP Conference Series, Vol 428. 287-295. https://www.aspbooks.org › publications › 428 › 287.pdf.

Adams, J. M., Piovesan, G., 2005. *Long series relationships between global interannual CO_2 increment and climate: Evidence for stability and change in role of the tropical and boreal-temperate zones*. Chemosphere, 59. 1595-1612. https://doi.org/10.1016/j.chemosphere.2005.03.064.

Ahn, J., Brook, E. J., Mitchell, L., Rosen, J., McConnell, J. R., Taylor K., Etheridge, D., Rubino, M., 2012, *Atmospheric CO_2 over the last 1000 years: A high-resolution record from the West Antarctic Ice Sheet (WAIS) Divide ice core.* Global Biogeocehmical Cycles, 26. GB2027, 1-11. https://doi.org/10.1029/2011GB004247.

Bard, E., Frank, M., 2006, *Climate change and solar variability: What's new under the sun?* Earth and Planetary Science Letters, 248, 1-2, 1-14. https://doi.org/10.1016/j.epsl.2006.06.016.

Bard, E., Raisbeck, G., Yiou, F., Jouzel, J., 2000. *Solar irradiance during the last 1200 years based on cosmogenic nuclides*. Tellus B: Chemical and Physical Meteorology, 52-3. 985-992. DOI: 10.3402/tellusb.v52i3.17080.

Benjamini, Y., Hochberg, Y., 1995. *Controlling the False Discovery Rate: A Practical and Powerful Approach to Multiple Testing*. Journal of the Royal Statistical Society: Series B (Methodological), 57(1), 289–300. https://www.jstor.org/stable/2346101.

Beran, J., 1994. *Statistics for long-memory processes.* Chapman and Hall. https://doi.org/10.1201/9780429488670.

Box, G. E., Jenkins, G. M., Reinsel, G. C., & Ljung, G. M. (2015). *Time Series Analysis: Forecasting and Control* (5th ed.). Wiley.

Bretherton, C. S., Smith, C., Wallace, J. M., 1999. *An Intercomparison of Methods for Finding Coupled Patterns in Climate Data*. Journal of Climate, 5(6), 541–560. https://doi.org/10.1175/1520-0442(1992)005<0541:AIOMFF>2.0.CO;2.

Breusch, T. S., 1978. *Testing for autocorrelation in dynamic linear models*. Australian Economic Papers, 17(31), 334–355. https://doi.org/10.1111/j.1467-8454.1978.tb00635.x.

Chapman and Hall/CRC. https://doi.org/10.1201/9781482295304.

Bielfeld, A., 2023, *The Tonga Eruption and its Effect on Earth.* News10NBC, November 29, 2023. https://www.whec.com/top-news/the-tonga-eruption-and-its-effect-on-earth/.

Caillon, N., Severinghaus, J. P., Jouzel, J., Barnola, J-M., Kang, J., Lipenkov, V. Y., 2003. *Timing of Atmospheric CO_2 and Antarctic Temperature Changes Across Glacial Terminations*. www.sciencemag.org, 299. 1728-1731. DOI: 10.1126/science.1078758.

Chow, G. C., 1960. *Tests of Equality Between Sets of Coefficients in Two Linear Regressions.* Econometrica, 28(3), 591–605. https://doi.org/10.2307/1910133.

Christy, J., Spencer, R., 2024a. *ESSC Global Temperature Report: August 2024*. The University of Alabama in Hunstville, 35, 5. 1-4. https://www.uah.edu/essc/weather-products/global-temperature-report.

Christy, J., Spencer, R., 2024b. *UAH Lower Troposphere Data, August 2024*. (accessed August 6, 2023). The University of Alabama in Hunstville. https://www.nsstc.uah.edu/data/msu/v6.0/tlt/uahncdc_lt_6.0.txt.

Chylek, P., Folland, C.K., Lesins, G., & Dubey, M.K., 2018a. *Ice core data evidence for a prominent near 20 year time lag of the Antarctic climate response to solar variability*. Geophysical Research Letters, 45, 11749–11756. https://doi.org/10.1029/2018GL079172.

Chylek, P., Tans, P., Christy, J., Dubey, M. K., 2018b. *The carbon cycle response to two El Nino types: an observational study*. Environmental Research Letters, 13. 024001, 1-8. DOI: 10.1088/1748-9326/aa9c5b.

Cobb, K. M., Charles, C. D., Cheng, H., Kastner, M. & Edwards, R. L. 2003. *El Niño/Southern Oscillation and tropical Pacific climate during the last millennium*. Nature 424, 271–276. DOI https://doi.org/10.1038/nature01779.

Covey, C., Thompson, S., Weissman, P., 1994, MacCracken, M., *Global Climatic Effects of Atmospheric Dust from an Asteroid or Comet Impact on Earth*. Global and Planetary Change, 10, 1-25. https://doi.org/10.1016/0921-8181(94)90020-5.

Cronin, T. M., Hayo, K., Thunell, R.C., Dwyer, G. S., Saenger, C., Willard, D.A., 2010. *The Medieval Climate Anomaly and Little Ice Age in Chesapeake Bay and the North Atlantic Ocean*. Palaeogeography, Palaeoclimatology, Palaeoecology, 297, 299-310. DOI: 10.1016/j.palaeo.2010.08.009.

Crowley, T. J., 2000. *Causes of Climate Change Over the Past 1000 Years*. Science, 289. 270-277. DOI: 10.1126/science.289.5477.270.

D'Aleo, J. S., Easterbrook, D. J., 2016. *Relationship of Multidecadal Global Temperatures to Multidecadal Oceanic Oscillations* (Chapter 11). In D. J. Easterbrook (Ed.), 2016. Evidence-Based Climate Science: Data Opposing CO_2 Emissions as the Primary Source of Global Warming (2^{nd} ed.). Elsevier, 418 pp. 191-214. https://doi.org/10.1016/B978-0-12-804588-6.00011-2

D'Aleo, J. S., 2016. *Solar Changes and the Climate* (Chapter 15). In D. J. Easterbrook (Ed.),

2016. Evidence-Based Climate Science: Data Opposing CO_2 Emissions as the Primary Source of Global Warming (2nd ed.). Elsevier, 418 pp. 263-282. DOI: xxx.

Davis, W. J., 2017. *The Relationship between Atmospheric Carbon Dioxide Concentration and Global Temperature for the Last 425 Million Years*. Climate, 5. 76, 1-34. DOI: 10.3390/cli5040076.

Dekan, K., 2021. *Volcanism and extreme climatic variability of the mid-13th century: Initiating the little Ice Age*, Little Ice Age. 1-9. DOI: 10.13140/RG.2.2.29018.36809.

Diebold, F. X., Rudebusch, G. D., 1991. *On the power of Dickey-Fuller tests against fractional alternatives*. Economics Letters, 35(2), 155–160. https://doi.org/10.1016/0165-1765(91)90067-T.

Doos, K., Nilsson, J., Nycander, J., Brodeau, L., Ballarotta, M., 2012. *The World Ocean Thermohaline Circulation*. Journal of Physical Oceanography, 42. 1445-1460. DOI: https://doi.org/10.1175/JPO-D-11-0163.1.

Douglass, D. H., Clader, B. D., 2002. *Climate sensitivity of the Earth to solar irradiance*. Geophysical Research Letters, 29. 16, 33-1-33-4. https://doi.org/10.1029/2002GL015345.

Douglass, D. H., Christy, J., 2009. *Limits on CO_2 Climate Forcing from Recent Temperature Data of Earth*. Energy and Environment, 20, 1&2. https://doi.org/10.1260/095830509787689277.

Durbin, J., Watson, G. S., 1950. *Testing for serial correlation in least squares regression: I.* Biometrika, 37(3/4), 409–428. https://doi.org/10.1093/biomet/37.3-4.409.

Easterbrook, D. J., 2016a. *Cause of Global Climate Changes: Correlation of Global Temperature, Sunspots, Solar Irradiance, Cosmic Rays, and Radiocarbon and Berylium Production Rates (Chapter 14)*. In D. J. Easterbrook (Ed.), 2016. Evidence-Based Climate Science: Data Opposing CO_2 Emissions as the Primary Source of Global Warming (2nd ed.). Elsevier, 418 pp. 245-262. https://doi.org/10.1016/B978-0-12-804588-6.00014-8.

Easterbrook, D. J., 2016b. *Greenhouse Gases (Chapter 9)*. In D. J. Easterbrook (Ed.), 2016. Evidence-Based Climate Science: Data Opposing CO_2 Emissions as the Primary Source of Global Warming (2nd ed.). Elsevier, 418 pp. 163-173. https://doi.org/10.1016/B978-0-12-385956-3.10019-1.

Ermoli, I., Matthes, K., Wit, D., Krivova, N., Tourpali, K., Weber, M., Unruh, Y., Gray, L., Langematz, U., Pilewskie, P., Rozanov, E., Schmutz, W., Shapiro, A., Solanki, S., Woods, T., 2013, *Recent variability of the solar spectral irradiance and its impact on climate modelling.* Atmospheric Chemistry and Physics Discussions, 13. 3945-3977. https://doi.org/10.5194/acp-13-3945-2013.

Esper, J., Cook, E., Schweingruber, F. H., 2002. *Low-Frequency Signals in Long Tree-Ring Chronologies for Reconstructing Past Temperature Variability*. Science, 295. 2250, 1-4. DOI: 10.1126/science.1066208.

Frank, D. C., Esper, J., Raible, C. C., Buntgen, U., Trouet, V., Stocker, B., Joos, F., 2010. *Ensemble reconstruction constraints on the global carbon cycle sensitivity to climate*. Nature, 463. 527-532. https://doi.org/10.1038/nature08769.

Gelman, A. & Hill, J. Data *Analysis Using Regression and Multilevel/Hierarchical Models*. (Cambridge Univ. Press, 2006). https://doi.org/10.1017/CBO9780511790942.

Geweke, J., Porter-Hudak, S., 1983. *The estimation and application of long memory time series models*. Journal of Time Series Analysis, **4**(4), 221–238. DOI: 10.1111/j.1467-9892.1983.tb00371.x.

Godfrey, L. G., 1978. *Testing for higher order serial correlation in regression equations when the regressors include lagged dependent variables*. Econometrica, 46(6), 1303–1310. https://doi.org/10.2307/1913835.

Gong, Y., Lu, J., Li, T., 2024. *The Impact of Annual Cycles on Anomalous Wind Meridional Structures of the ENSO*. Atmosphere, 15. 940, 1-10. DOI: 10.3390/atmos15080950.

Granger, C. W. J., 1969. *Investigating Causal Relations by Econometric Models and Cross-spectral Methods*. Econometrica, 37(3), 424–438. DOI: 10.2307/1912791.

Granger, C. W. J., & Newbold, P. (1974). *Spurious regressions in econometrics*. Journal of Econometrics, 2(2), 111–120. https://doi.org/10.1016/0304-4076(74)90034-7.

Granger, C. W. J., Joyeux, R., 1980. *An introduction to long-memory time series models and fractional differencing*. Journal of Time Series Analysis, 1(1), 15–29. https://doi.org/10.1111/j.1467-9892.1980.tb00297.x.

Gray, L. J., Beer, J., Geller, M., Haigh, J. D., Lockwood, M., Matthes, K., Cubasch, U., Fleitmann, D., Harrison, G., Hood, L., Luterbacher, J., Meehl, G. A., Shendell, D., van Geel, B., White, W., 2010. *Solar Influences on Climate*. Reviews of Geophysics, 48. RG4001, 1-53. https://doi.org/10.1029/2009RG000282.

Gray, S. T., Betancourt, J. L., Fastie, C. L., Jackson, S. T., 2003. *Patterns and sources of multidecadal oscillations in drought-sensitive tree-ring records from the central and southern Rocky Mountains*. Geophysical Research Letters, 30. 49, 1-4. DOI: 10.1029/2002GL016154.

Gray, W. M., 2012, *The Physical Flaws of the Global Warming Theory and Deep Ocean Circulation Changes as the Primary Climate Driver*. The Heartland Institute 7th International Conference on Climate Change (ICCC-7). 1-32. http://tropical.atmos.colostate.edu/Includes/Documents/Publications/gray2012.pdf.

Haigh, J., Winning, A., Toumi, R., Harder, J., 2010. *An influence of solar spectral variations on radiative forcing of climate*. Nature, 467. 696-699. https://doi.org/10.1038/nature09426.

Harris, C. R., Millman, K. J., van der Walt, S. J., Gommers, R., Virtanen, P., Cournapeau, D. et al., 2020. *Array programming with NumPy*. Nature, 585, 357–362. https://doi.org/10.1038/s41586-020-2649-2.

Hegerl, G. C., Crowley, T. J., Allen, M., Hyde, W. T., Pollack, H. N., Smerdon, J., Zorita, E., 2007. *Detection of Human Influence on a New, Validated 1500-Year Temperature Reconstruction*. Journal of Climate, 20. 650-666. https://doi.org/10.1175/JCLI4011.1.

Hoesly, R. M., Smith, S. J., Feng, L., Kilmont, Z., Janssens-Maenhout, G., Pitkanen, T., Selbert, J. J., Vu, L., Andres, R. J., Bolt, R. M., Bond, T. C., Dawidowski, L., Kholod, N., Kurokawa, J., Li, M., Liu, L., Lu, Z., Moura, M. C. P., O'Rourke, R., Zhang, Q., 2018. *Historical (1750–2014) anthropogenic emissions of reactive gases and aerosols from the Community Emissions Data System (CEDS)*. Geoscientific Model Development, 11, 369-408. https://doi.org/10.5194/gmd-11-369-2018.

Hoyt, D. V., Schatten, K. H., 1993. *A Discussion of Plausible Solar Irradiance Variations, 1700-1992.* Journal of Geophysical Research, 98. 18,895-18,906. https://doi.org/10.1029/93JA01944.

Hoyt, D. V., Schatten, K. H., 1997. *The Role of the Sun in Climate Change*. Oxford University Press, 279 pp. https://doi.org/10.1023/A:1006179829911.

Hunter, J. D., 2007. *Matplotlib: A 2D graphics environment*. Computing in Science & Engineering, 9 (3), 90–95. https://doi.org/10.1109/MCSE.2007.55.

Hyndman, R. J., & Athanasopoulos, G. (2018). *Forecasting: Principles and Practice* (2nd ed.). OTexts. https://otexts.com/fpp2/

Humlum, O., Stordahl, K., Solheim, J-E., 2013. *The phase relation between atmospheric carbon dioxide and global temperature*. Global and Planetary Change, 100. 51-69. http://dx.doi.org/10.1016/j.gloplacha.2012.08.008.

Hurst, H. E., 1951. *Long-term storage capacity of reservoirs*. Transactions of the American

Society of Civil Engineers, 116, 770–799.

Huybers, P. J., & Curry, W. B. (2006). *Links between annual, Milankovitch and continuum temperature variability*. Nature, 441(7091), 329–332. https://doi.org/10.1038/nature04745.

Imbrie, J., Boyle, E. A., Clemens, S. C., Duffy, A., Howard, W. R., Kukla, G., Kutzbach, J., Martinson, D. G., McIntyre, A., Mix, A. C., Molfino, B., Moreley, J. J., Peterson, L. C., Pisias, N. G., Prell, W. L., Raymo, M. E., Shackleton, N. J., Toggweiler, J. R., 1992. *On the Structure and Origin of Major Glaciation Cycles 1. Linear Responses to Milankovitch Forcing*. Paleoceanography, 7, 6, 701-738. https://doi.org/10.1029/92PA02253.

Ineson, S., Scaife, A. A., Knight, J. R., Manners, J. C., Dunstone, N. J., Gray, L. J., Haigh, J. D., 2011. *Solar forcing of winter climate variability in the Northern Hemisphere*. Nature Geoscience, 4. 753-757. https://doi.org/10.1038/ngeo1282.

James, G., Witten, D., Hastie, T., & Tibshirani, R. (2021). *An Introduction to Statistical Learning* (2nd ed.). Springer. https://doi.org/10.1007/978-1-0716-1418-1.

Jones, P. D., Briffa, K. R., Barnett, T. P., Tett, S. F. B., 1998. *High-resolution palaeoclimatic records for the last millennium: interpretation, integration and comparison with General Circulation Model control-run temperatures*. The Holocene, 8. 4, 455-471. https://doi.org/10.1191/095968398667194956.

Jones, P. D., & Mann, M. E. (2004). *Climate over past millennia*. Reviews of Geophysics, 42(2). https://doi.org/10.1029/2003RG000143

Juckes, M. N., Allen, M. R., Briffa, K. R., Esper, J., Hegerl, G. C., Moberg, A., Osborn, T. J., Weber, S. L., 2007. *Millennial temperature reconstruction intercomparison and evaluation*. Climate of the Past, 3. 591-609. https://doi.org/10.5194/cp-3-591-2007.

Katata, G., Connolly, R., O'Neill, P., 2023. *Evidence of Urban Blending in Homogenized Temperature Records in Japan and in the United States: Implications for the Reliability of Global Land Surface Air Temperature Data*. Journal of Applied Meteorology and Climatology, 62. 1095-1114. DOI: 10.1175/JAMC-D-22-0122.1.

Kennedy J.J., Rayner, N.A., Smith, R.O., Saunby, M. and Parker, D.E. (2011a). *Reassessing biases and other uncertainties in sea-surface temperature observations since 1850 part 1: Measurement and sampling errors*. J. Geophys. Res., 116, D14103, doi:10.1029/2010JD015218 (PDF 1Mb) (accessed August 6, 2023). https://www.metoffice.gov.uk/hadobs/hadsst3/data/HadSST.3.1.1.0/diagnostics/HadSST.3.1.1.0_annual_globe_ts.txt.

Kennedy J.J., Rayner, N.A., Smith, R.O., Saunby, M. and Parker, D.E. (2011b). *Reassessing biases and other uncertainties in sea-surface temperature observations since 1850 part 2: Biases and homogenization*. J. Geophys. Res., 116, D14104, doi:10.1029/2010JD015220. (PDF 1Mb) (accessed August 6, 2023). https://www.metoffice.gov.uk/hadobs/hadsst3/data/HadSST.3.1.1.0/diagnostics/HadSST.3.1.1.0_annual_globe_ts.txt.

Komitov, B., Kaftan, V., 2020. *The Volcanic and Solar Activity Relationship During the Last ~ 460 Years. Could a Significant Part of the "Sun-Climate" Relationship Goes Through Lithosphere?* In Georgieva, K., Kirov, B., Danov, D., 2020. Workshop "Solar Influences on the Magnetosphere, Ionosphere and Atmosphere", Book of Proceedings. Space Research and Technologies Institute Bulgarian Academy of Sciences, 135-140. DOI: 10.31401/WS.2020.proc.

Koscielny-Bunde, E., Bunde, A., Havlin, S., Roman, H. E., Goldreich, Y., Schellnhuber, H. J., 1998. *Indication of a universal persistence law governing atmospheric variability.* Physical Review Letters, 81(3), 729–732. https://doi.org/10.1103/PhysRevLett.81.729.

Koskinas, A., Zacharopoulou, E., Pouliasis, G., Deligiannis, I., Dimitriadis, P., Iliopoulou, T., Mamassis, N., and Koutsoyiannis, D., 2022. *Estimating the Statistical Significance of*

Cross–Correlations between Hydroclimatic Processes in the Presence of Long–Range Dependence, Earth, 3 (3), 1027-1041, doi:10.3390/earth3030059, 2022.

Kouwenberg, L., Wagner, R., Kurschner, W., Visscher, H., 2005, *Atmospheric CO_2 fluctuations during the last millennium reconstructed by stomatal frequency analysis of Tsuga heterophylla needles*. Geological Society of America, 33, No. 1, 33-36.

Koutsoyiannis, D., 2024a, *Stochastic assessment of temperature – CO_2 causal relationship in climate from the Phanerozoic through modern times*, Mathematical Biosciences and Engineering, 21 (7), 6560–6602, doi:10.3934/mbe.2024287.

Koutsoyiannis, D., 2024b, *The relationship between atmospheric temperature and carbon dioxide concentration*, Science of Climate Change, 4 (3), 39–59, doi:10.53234/scc202412/15, 2024b.

Koutsoyiannis, D., 2024c, *Stochastics of Hydroclimatic Extremes - A Cool Look at Risk*, Edition 4, ISBN: 978-618-85370-0-2, 400 pages, doi:10.57713/kallipos-1, Kallipos Open Academic Editions, Athens.

Koutsoyiannis, D. and Kundzewicz, Z. W., 2020, *Atmospheric temperature and CO_2: Hen-or-egg causality?*, Sci, 2 (4), 83, doi:10.3390/sci2040083.

Koutsoyiannis, D., Onof, C., Christofides, A., and Kundzewicz, Z. W., 2022a, *Revisiting causality using stochastics: 1.Theory*, Proceedings of The Royal Society A, 478 (2261), 20210835, doi:10.1098/rspa.2021.0835.

Koutsoyiannis, D., Onof, C., Christofides, A., and Kundzewicz, Z. W., 2022b, *Revisiting causality using stochastics: 2*. Applications, Proceedings of The Royal Society A, 478 (2261), 20210836, doi:10.1098/rspa.2021.0836.

Koutsoyiannis, D., Onof, C., Kundzewicz, Z. W., and Christofides, A., 2023, *On hens, eggs, temperatures and CO_2: Causal links in Earth's atmosphere*, Sci, 5 (3), 35, doi:10.3390/sci5030035.

Knudsen, M. F., Seidenkrantz, M. S., Jacobsen, B. H., Kuijpers, A., 2011. *Tracking the Atlantic Multidecadal Oscillation through the last 8,000 years.* Nature Communications, 10. 1038, Trenberth 1-9. https://doi.org/10.1038/ncomms1186.

Lean, J., 2000. *Evolution of the Sun's Spectral Irradiance Since the Maunder Minimum.* Geophysical Research Letters, 27. 16, 2425-2428. https://doi.org/10.1029/2000GL000043.

Lean, J. L., 2018. *Estimating Solar Irradiance Since 850 CE*. Earth and Space Science, 5. 133-149. https://doi.org/10.1002/2017EA000357.

Lee, J. and Wang, A., 2022. *Tonga Eruption Blasted Unprecedented Amount of Water Into Stratosphere*, August 2, 2022. Jet Propulsion Laboratory. https://www.nasa.gov/earth/tonga-eruption-blasted-unprecedented-amount-of-water-into-stratosphere/.

Lenssen, N., G.A. Schmidt, M. Hendrickson, P. Jacobs, M. Menne, and R. Ruedy, 2024: *A GISTEMPv4 observational uncertainty ensemble.* J. Geophys. Res. Atmos., 129, no. 17, e2023JD040179, doi:10.1029/2023JD040179.
https://data.giss.nasa.gov/gistemp/tabledata_v4/GLB.Ts+dSST.txt.

Li, Z., Chang, L., Lou, J., Shen, Y., Yan, H., 2022. *Multi-scale Analysis of the Relationships between Solar Activity, CO_2 and Global Surface Temperature*. Research in Astronomy and Astrophysics, 22. DOI 10.1088/1674-4527/ac8339.

Lin, J., Qian, T., 2022. *The Atlantic Multi-Decadal Oscillation*. Atmosphere-Ocean, 60. 3-4, 307-337. https://doi.org/10.1080/07055900.2022.2086847.

Ljung, G. M., Box, G. E. P., 1978. *On a measure of lack of fit in time series models.* Biometrika,

65(2), 297–303. https://doi.org/10.1093/biomet/65.2.297.

Ljungqvist, F. C., 2010, *A New Reconstruction of Temperature Variability in the Extra-Tropical Northern Hemisphere During the last Two Millennia*. Swedish Society for Anthropology and Geography, Series A. Sept 6. https://doi.org/10.1111/j.1468-0459.2010.00399.x.

Lockwood, M., Stamper, R., 1999. *Long-term drift of the coronal source magnetic flux and the total solar irradiance*. Geophysical Research Letters, 26. 16, 2461-2464. https://doi.org/10.1029/1999GL900485.

Loehle, C., McCulloch, J. H., 2008. *Correction to: A 2000-Year Global Temperature Reconstruction Based on Non-Tree Ring Proxies.* Energy & Environment, 19. 1, 92-100. https://www.jstor.org/stable/44397366.

Lorenz, S. J., Kim, J., Rimbu, N, Schneider, R. R., Lohmann, G., 2006. *Orbitally driven insolation forcing on Holocene climate trends: Evidence from alkenone data and climate modeling*. Paleoceanography, 21. PA1002. doi:10.1029/2005PA001152.

Lourens, L. J., Tuenter, E., 2016. *Chapter 25 – The Variation of the Earth's Movements (Orbital, Tilt and Precession)*. In T. Letcher (Ed.) Climate Change – Observed Impacts on Planet Earth (2nd ed.). Elsevier, 632 pp. 399-418. https://doi.org/10.1016/B978-0-444-63524-2.00025-7.

MacFarling Meure, C., Etheridge, D., Trudinger, C., Steele, P., Langenfelds, R., van Ommen, T., Smith, A., Elkins, J., 2006. *Law Dome CO_2, CH4 and N2O ice core records extended to 2000 years BP*. Geophysical Research Letters, 33. L14810, 1-5. https://doi.org/10.1029/2006GL026152.

Mann, M.E., Bradley, R.S., & Hughes, M.K., 1999. *Northern Hemisphere temperatures during the past millennium: Inferences, uncertainties, and limitations.* Geophysical Research Letters, 26(6), 759–762. https://doi.org/10.1029/1999GL900070.

Mann, M. E. (2004). *On smoothing potentially non-stationary climate time series*. Geophysical Research Letters, 31(7). https://doi.org/10.1029/2004GL019569.

Mann, M. E., Zhang, Z., Hughes, M. K., Bradley, R. S., Miller, S. K., Rutherford, S., Ni, F., 2008. *Proxy-based reconstructions of hemispheric and global surface temperature variations over the past two millennia*. Proceedings of the National Academy of Sciences, 105. 36, 1-6. https://doi.org/10.1073/pnas.0805721105.

Mann, M. E., Zhang, Z., Rutherford, S., Bradley, R. S., Hughes, M. K., Shindell, D., Ammann, C., Faluvegi, G., Ni, F., 2009. *Global Signatures and Dynamical Origins of the Little Ice Age and Medieval Climate Anomaly*. Science, 326. 1256-1260. DOI: 10.1126/science.1177303.

Marsh, G. E., 2014, *Interglacials, Milankovitch Cycles, Solar, Activity, and Carbon Dioxide*. Journal of Climatology, 2014. 345482, 1-7. https://doi.org/10.1155/2014/345482.

McGregor, H. V., Evans, M. N., Goosse, H., Leduc, G., Martrat, B., Addison, J. A., Mortyn, P. G., Oppo, D. W., Seidenkrantz, M. S., Sicre, M.-A., & Waelbroeck, C., 2013. *Robust global ocean cooling trend for the pre-industrial Common Era.* Nature Geoscience, 6(7), 615–620. DOI: 10.1038/ngeo1797.

McKinney, W., 2010. *Data structures for statistical computing in Python*. Proceedings of the 9th Python in Science Conference, 51–56. https://doi.org/10.25080/Majora-92bf1922-00a.

McKitrick, R., 2010. *A Critical Review of Global Surface Temperature Data Products*. SSRN, 6 August 2010. https://papers.ssrn.com/sol3/papers.cfm?abstract_id=1653928.

Middleton, D., 2011. *CO_2: Ice Cores vs. Plant Stomata*. https://wattsupwiththat.com/2010/12/26/co2-ice-cores-vs-plant-stomata/.

Microsoft Corporation, 2022. *Microsoft Excel, Version 2301, with Visual Basic for Applications*. Redmond, WA: Microsoft Corporation.

Moberg, A., Sonechkin, D. M., Holmgren, K., Datsenko, N. M., Karlen, W., 2005. *Highly variable Northern Hemisphere temperatures reconstructed from low- and high-resolution proxy data.* Nature, 3265. 1-5. DOI: 10.1038/nature03265.

Moffa-Sanchez, P., Born, A., Hall, I. R., Thornalley, D. J. R., Barker, S., 2014. *Solar forcing of North Atlantic surface temperature and salinity over the past millennium*. Nature Geoscience, 7. 275-278. https://doi.org/10.1038/ngeo2094.

Monnin, E., Indermuhle, A., Dallenbach., A, Fluckiger, J., Stauffer, B., Stocker, T. F. Raynaud, D., Barnola, J-M., 2001. *Atmospheric CO_2 Concentrations over the Last Glacial Termination.* www.sciencemag.org, 291. 112-114. DOI: 10.1126/science.291.5501.112.

Morice, C. P., J. J. Kennedy, N. A. Rayner, and P. D. Jones, 2012, *Quantifying uncertainties in global and regional temperature change using an ensemble of observational estimates: The HadCRUT4 dataset*. J. Geophys. Res., 117, D08101. (accessed August 6, 1923) doi:10.1029/2011JD017187.https://www.metoffice.gov.uk/hadobs/hadcrut4/data/current/time_series/HadCRUT.4.6.0.0.annual_ns_avg.txt.

Morner, N., 2012. *Planetary beat, solar wind and terrestrial climate*. In Borrega, C. D. E. and Cruz, A. F. B. (Ed.), 2012. Solar Wind: Emission, Technologies and Impacts. Nova Science Publishers. Inc., 987 pp. 47-66. https://novapublishers.com/shop/solar-wind-emission-technologies-and-impacts/.

Mudelsee, M., 2001. *The phase relations among atmospheric CO_2 content, temperature and global ice volume over the past 420 ka*. Quaternary Science Reviews, 20. 583-589. https://doi.org/10.1016/S0277-3791(00)00167-0. DOI 10.1007/s11207-016-0969-z.

Mudelsee, M., 2010. *Climate Time Series Analysis: Classical Statistical and Bootstrap Methods*. Springer. https://doi.org/10.1007/978-90-481-9482-7.

Mudelsee, M., 2014. Climate Time Series Analysis: Classical Statistical and Bootstrap Methods (2nd ed.) Springer. DOI: 10.1007/978-3-319-04450-7.

Muscheler, R., Adolphi, F., Herbst, K., Nilsson, A., 2016. *The Revised Sunspot Record in Comparison to Cosmogenic Radionuclide-Based Solar Activity Reconstructions*. Solar Physics, 291. 3025-3043.

Newey, W.K. and West, K.D. (1987) A simple, positive semi-definite, heteroskedasticity and autocorrelation consistent covariance matrix. Econometrica, 55(3), 703-708. DOI 10.3386/t0055.

Ogurtson, M. G., Nagovitsyn, A., Kocharov, G. E., Jungner, H., 2002. *Long-period cycles of the sun's activity recorded in direct solar data and proxies.* Solar Physics, 211. 371-394. https://doi.org/10.1023/A:1022411209257.

Parker, D.E., T.P. Legg, and C.K. Folland. 1992. *A new daily Central England Temperature Series*. 1772-1991. Int. J. Clim., Vol 12, pp 317-342 (PDF) (accessed August 6, 2023) https://www.metoffice.gov.uk/hadobs/hadcet/data/legacy/cetml1659on.dat.

Pearson, K., 1896. *Mathematical contributions to the theory of evolution. III. Regression, heredity, and panmixia*. Philosophical Transactions of the Royal Society of London. A, 187, 253–318. https://doi.org/10.1098/rsta.1896.0007.

Peltier Tech, 2024. Peltier Technical Services. Peltier Tech Website (https://peltiertech.com/documentation/loess/).

Peng, C. K., Buldyrev, S. V., Havlin, S., Simons, M., Stanley, H. E., & Goldberger, A. L., 1994. *Mosaic organization of DNA nucleotides*. Physical Review E, 49(2), 1685–1689. https://doi.org/10.1103/PhysRevE.49.1685.

Politis, D. N., & Romano, J. P., 1994. *The Stationary Bootstrap*. Journal of the American Statistical Association, 89(428), 1303–1313. DOI: 10.1080/01621459.1994.10476870.

Python Software Foundation, 2023. *Python Language Reference, version 3.10.*

https://www.python.org.

Quintessa Limited, 2020. *Graph Grabber v2.0.2*.

R Core Team, 2024. *R: A language and environment for statistical computing*. R Foundation for Statistical Computing, Vienna, Austria. https://www.R-project.org.

Roe, G., 2006. *In defense of Milankovitch.* Geophysical Research Letters, 33, L24703, 1-5. DOI: 10.1029/2006GL027817.

Rubino, M., Etheridge, D. M., Thornton, D. P., Howden, R., Allison, C. E., Francey, R. J., Langenfelds, R. L., Steele, L. P., Trudinger, C. M., Spencer, D. A., Curran, M. A. J., Ommen, T. D., Smith, A. M., 2019. *Revised records of atmospheric trace gases CO_2, CH4, N2O, and δ 13C-CO_2 over the last 2000 years from Law Dome, Antarctica.* Earth Systems Science Data, 11, 473-492. https://doi.org/10.5194/essd-11-473-2019.

Scafetta, N., 2021. *Detection of non-climatic biases in land surface temperature records by comparing climatic data and their model simulations.* Climate Dynamics, 56. 2959-2982. https://doi.org/10.1007/s00382-021-05626-x.

Scafetta, N., Bianchini, A., 2022. *The Planetary Theory of Solar Activity Variability: A Review*. Frontiers in Astronomy and Space Sciences, 9. 937930, 1-26. https://doi.org/10.3389/fspas.2022.937930.

Scafetta, N., 2023. *Empirical assessment of the role of the Sun in climate change using balanced multi-proxy solar records*. Geoscience Frontiers, 14. 101650, 1-19. https://doi.org/10.1016/j.gsf.2023.101650.

Schwander, M., Rohrer, M., Bronnimann, S., Malik, A., 2017. *Influence of solar variability on the occurrence of central European weather types from 1763 to 2009*. Climate of the Past, 13. 1199-1212. https://doi.org/10.5194/cp-13-1199-2017.

Schmutz, W. K., 2021. *Changes in the Total Solar Irradiance and climatic effects.* Journal Space Weather Space Climate, 11. 40, 1-13. https://doi.org/10.1051/swsc/2021016.

Shackleton, N. J., 2000. *The 100,000-Year Ice-Age Cycle Identified and Found to Lag Temperature, Carbon Dioxide, and Orbital Eccentricity*. Science, 289. 1897-1902. DOI: 10.1126/science.289.5486.1897.

Shapiro, A. I., Schmutz, W., Rozanov, E., Schoell, M., Haberreiter, M., Shapiro, A. V., Nyeki, S., 2011. *A new approach to the long-term reconstruction of the solar irradiance leads to large historical solar forcing*. Astronomy & Astrophysics, 529. A67, 1-8. https://doi.org/10.48550/arXiv.1102.4763.

Sharma, K., Karamanev, D., 2021. *Investigating the Historic Correlation between Atmospheric Carbon Dioxide Concentration and Global Temperature Change*. Ecological Engineering and Environmental Protection, 1. 5-16. DOI: 10.32006/eeep.2021.1.0516.

Shaviv, N. J., 2008. *Using the oceans as a calorimeter to quantify the solar radiative forcing*. Journal of Geophysical Research, 113. A11101, 1-13. doi:10.1029/2007JA012989.

Shaviv, N. J., Svensmark, H., Veizer, J., 2023, *The Phanerozoic climate*. Annals of the New York Academy of Sciences, 1519. 7-19. https://doi.org/10.1111/nyas.14920.

Solanki, S., Fligge, M., 1999, *A reconstruction of total solar irradiance since 1700.* Geophysical Research Letters, 26. 16, 2465-2468. https://doi.org/10.1029/1999GL900370.

Soon, W. H., 2009. *Solar Arctic-mediated Climate Variation on Multidecadal to Centennial Timescales: Empirical Evidence, Mechanistic Explanation, and Testable Consequences.* Physical Geography, 30. 144-184. https://doi.org/10.2747/0272-3646.30.2.144.

Soon, W., Connolly, R., Connolly, M., 2015. *Re-evaluating the role of solar variability on Northern Hemisphere temperature trends since the 19th century*. Earth-Science Reviews, 150. 409-

452. https://doi.org/10.1016/j.earscirev.2015.08.010.

Soon, W., Legates, D. R., 2013. *Solar irradiance modulation of Equator-to-Pole (Arctic) temperature gradients: Empirical evidence for climate variation on multi-decadal timescales.* Journal of Atmospheric and Solar-Terrestrial Physics, 93. 25-56. https://doi.org/10.1016/j.jastp.2012.11.015.

Soon, W., Connolly, R., Connolly, M., Akasofu, S., Baliunas, S., Berglund, J., Bianchini, A., Briggs, W., Butler, C., Cionco, R., Crok, M., Elias, A., Fedorov, V., Gervais, F., Harde, H., Henry, G., Hoyt, D., Humlum, O., Legates, D., Lupo. A., Maruyama, S., Moore, P., Ogurtsov, M., ÓhAiseadha, C., Oliveira, M., Park, S., Qiu, S., Quinn, G., Scafetta, N., Solheim, J., Steele, J., Szarka, L., Tanaka, H., Taylor, M. Vahrenholt, F., Velasco Herrera, V., Zhang, W., 2023. *The Detection and Attribution of Northern Hemisphere Land Surface Warming (1850–2018) in Terms of Human and Natural Factors: Challenges of Inadequate Data*. Climate, 11, 179. 1-36. https://doi.org/10.3390/cli11090179.

Spencer, R., 2024. *Recent UAH Research: Urban Heat Island Effects*. The University of Alabama in Huntsville. https://www.drroyspencer.com/2023/11/examples-from-our-new-uah-urban-heat-island-dataset/, June 15, 2024.

Stefani, F., Giesecke, A., Seilmayer, M., Stepanov, R., Weier, T., 2004. *Schwabe, Gleissberg, Suess-de Vries: Towards a Consistent Model of Planetary Synchronization of Solar Cycles*. Magnetohydrodynamics, 40. 1, 1-11. https://doi.org/10.48550/arXiv.1910.10383.

Steinhilber, F., Abreu, J. A., Beer, J, McCracken, K. G., 2010. *Interplanetary magnetic field during the past 9300 years inferred from cosmogenic radionuclides*. Journal of Geophysical Research, 115. A01104, 1-15.

Steinhilber, F., Beer, J., Frohlich, C., 2009. *Total solar irradiance during the Holocene*. Geophysical Research Letters, 36. L19704, 1-5. https://doi.org/10.1029/2009JA014193.

Stock, J. H., & Watson, M. W., 2003. *Introduction to Econometrics*. Addison-Wesley, Boston. 785 pp.

Svensmark, H., Friis-Christensen, E., 1997. Variation of cosmic ray flux and global cloud coverage-a missing link in solar-climate relationships. Journal of Atmospheric and Solar-Terrestrial Physics, 59. 11, 1225-1232. https://doi.org/10.1016/S1364-6826(97)00001-1

Svensmark, H., 1999. *Cosmic Rays and Earth's Climate*. Space Science Reviews, 93. 175-185. https://doi.org/10.1023/A:1026592411634.

Svensmark, H., 2007. *Cosmoclimatology: a new theory emerges*. Astronomy & Geophysics, 48. 1.18-1.24. https://doi.org/10.1111/j.1468-4004.2007.48118.x.

Svensmark, J., Enghoff, M. B., Shaviv, N. J., Svensmark, H., 2016. *The response of clouds and aerosols to cosmic ray decreases*. Journal of Geophysical Research: Space Physics, 121. 8152-8181. https://doi.org/10.1002/2016JA022689.

Svensmark, H., Svensmark, J., Enghoff, M. B., Shaviv, N. J., 2021. *Atmospheric ionization and cloud radiative forcing*. Scientific Reports, 11. 19668, 1-13. DOI: 10.1038/s41598-021-99033-1.

Svensmark, H., 2022. *Supernova Rates and Burial of Organic Matter*. Geophysical Research Letters, 48, e2021GL096376, 1-9. https://doi.org/10.1029/2021GL096376.

Toggweiler, J. R., Key, R. M., 2001. *Thermohaline Circulation*. Academic Press. 8 pp. https://doi.org/10.1016/B0-12-227090-8/00281-5.

Trenberth, K. E., 2016. *El Nino Southern Oscillation (ENSO)*. Elsevier, 12 pp. 1-12. https://doi.org/10.1016/B978-0-12-409548-9.04082-3.

US Historical Climatological Network, 2024, https://www.ncei.noaa.gov/data/ushcn/v25/.

Usoskin, I. G., Schussler, M., Solanki, S. K., Mursula, K., 2005. Solar activity, cosmic rays, and Earth's temperature: A millennium-scale comparison. Journal of Geophysical Research, 110. A10102, 1-11. https://doi.org/10.1029/2004JA010946.

Usoskin, I. G., Gallet, Y., Lopes, F., Kovaltsov, G. A., Hulot, G., 2016. *Solar activity during the Holocene: the Hallstatt cycle and its consequence for grand minima and maxima*. Astronomy & Geophysics, 587. A150, 1-10. DOI: 10.1051/0004-6361/201527295.

Vevard, C., Veizer, J., 2019. *On plate tectonics and ocean temperatures.* Geology, 47. 9, 881-885. https://doi.org/10.1130/G46376.1.

Vinos, J., 2024a, *Hunga-Tonga volcano: impact on record warming*. In Curry, J. A. (Ed), Climate Etc., https://judithcurry.com/2024/07/05/hunga-tonga-volcano-impact-on-record-warming/. July 5, 2024.

Vinos, J., 2024b, *Hunga Tonga volcano: impact on record warming*, in Watts, A., (Ed), Watts Up With That. https://wattsupwiththat.com/2024/07/09/hunga-tonga-volcano-impact-on-record-warming/. July 9, 2024.

Virtanen, P., Gommers, R., Oliphant, T. E., Haberland, M., Reddy, T., Cournapeau, D. et al., 2020. *SciPy 1.0: Fundamental algorithms for scientific computing in Python*. Nature Methods, 17 (3), 261–272. https://doi.org/10.1038/s41592-019-0686-2.

von Storch, H., Zwiers, F. W., 1999. *Statistical analysis in climate research.* Cambridge University Press. https://doi.org/10.1017/CBO9780511612336.

Wallace, J., D'Aleo, J., Idso, C., 2017. *On the Validity of NOAA, NASA and Hadley CRU Global Average Surface Temperature Data & The Validity of EPA's CO_2 - Endangerment Finding - Abridged Research Report*. Academia. https://www.academia.edu/33850726/On_the_Validty_of_NOAA_NASA_and_Hadley_CRU_Global_Average_Surface_Temperature_Data_and_The_Validity_of_EPAs_CO_2_Endangerment_Finding_Abridged_Research_Report. June, 2017.

Wang, G., Zhao, C., Zhang, M., Zhang, Y., Lin, M., Qiao, F., 2020. *The causality from solar irradiation to ocean heat content detected via multi-scale Liang–Kleeman information flow.* Scientific Reports, Nature Portfolio, 10. 17141, 1-9. https://doi.org/10.1038/s41598-020-74331-2.

Wang, Q., Ren, F., Li, R., 2024. *Uncovering the world's largest carbon sink—a profile of ocean carbon sinks research*. Environmental Science and Pollution Research, 31. 20362-20382. DOI: 10.1007/s11356-024-32161-z.

Wanner, H., Pfister, C., Neukom, R., 2022. *The variable European Little Ice Age*. Quaternary Science Reviews, 287. 107531. https://doi.org/10.1016/j.quascirev.2022.107531.

Watts, A. 2012, *An area and distance weighted analysis of the impacts of station 1 exposure on the U.S. Historical Climatology Network temperatures and 2 temperature trends.* In Watts, A. (Ed), Watts Up With That. https://wattsupwiththat.com/2012/07/29/press-release-2/. July 29, 2012.

White, W. B., Lean, J., Cayan, D. R., Dettinger, M. D., 1997. *Response of global upper ocean temperature to changing solar irradiance*. Journal of Geophysical Research, 102. C2, 3255-3266. https://doi.org/10.1029/96JC03549.

White, W. B., Dettinger, M. D., Cayan, D. R., 2000. *Global Average Upper Ocean Temperature Response to Changing Solar Irradiance: Exciting the Internal Decadal Mode.* Proceedings 1st Solar & Space Weather Euroconference. 125-132.

Wickham, H., 2016. *ggplot2: Elegant graphics for data analysis.* Springer-Verlag, New York. https://ggplot2.tidyverse.org.

Willson, R. C., Hudson, H. S., 1988. *Solar luminosity variations in solar cycle 21*. Nature, 332. 6167, 810-812. https://doi.org/10.1038/332810a0.

Willson, R. C., 1997. *Total Solar Irradiance Trend During Solar Cycles 21 and 22.* Science, 277. 1963-1965. DOI: 10.1126/science.277.5334.1963.

Willson, R. C., Mordvinov, A. V., 2003. *Secular total solar irradiance trend during solar cycles 21–23*. Geophysical Research Letters, 30. No. 5, 1199, 3-1 to 3-4. https://doi.org/10.1029/2002GL016038.

Wilson, Daniel C. S., 2014, *"Arnold Toynbee and the Industrial Revolution: The Science of History, Political Economy and the Machine Past."* History and Memory, vol. 26, no. 2, 2014, pp. 133–61. JSTOR, https://doi.org/10.2979/histmemo.26.2.133.

Wu, C. J., Krivova, N. A., Solanki, S. K., Usoskin, I. G., 2018. *Solar total and spectral irradiance reconstruction over the last 9000 years.* Astronomy & Astrophysics. 1-12. https://doi.org/10.1051/0004-6361/201832956.

Yang, B., Braeuning, A., Johnson, K. R., Yafeng, S., 2002. *General characteristics of temperature variation in China during the last two millennia*. Geophysical Research Letters, 29. No 9, 1324. 1-4. https://doi.org/10.1029/2001GL014485.

Yu, J., Anderson, R. F., Jin, Z. D., Ji, X., Thornalley, D. J. R., Wu, L., Thouveny, N., Cai, Y., Yan, L., Zhang, F., Menviel, L., Tian, J., Xie, X., Rohling, E. J., McManus, J. F., 2023. *Millennial atmospheric CO_2 changes linked to ocean ventilation modes over past 150,000 years*. Nature Geoscience, 16. 1166-1173. https://doi.org/10.1038/s41561-023-01297-x.

Zeileis, A., and Hothorn, T., 2002. *Diagnostic checking in regression relationships*. R News, 2 (3), 7–10. https://CRAN.R-project.org/package=lmtest.

Zeileis, A., and Grothendieck, G., 2005. *zoo: S3 infrastructure for regular and irregular time series*. Journal of Statistical Software, 14 (6), 1–27. https://doi.org/10.18637/jss.v014.i06.

Zhao, X., Soon, W., Herrera, V. M V., 2020. *Evidence for Solar Modulation on the Millennial-Scale Climate Change of Earth*. Universe, 6. 153, 1-9. https://doi.org/10.3390/universe6090153.

Copyright References

Figure 1. Copyright note - Figure reproduced with permission from: (1) Rubino et al. (2019) – © CC By 4.0; (2) Ljungqvist (2010) - © The authors 2010, Geografiska Annaler: Series A © 2010 Swedish Society for Anthropology and Geography reprinted by permission of Informa UK Limited, trading as Taylor & Francis Group, www.tandfonline.com om behalf of Swedish Society for Anthropology and Geography.

Figure 2. Copyright note - Figure reproduced with permission from: (1) Rubino et al. (2019) – © CC By 4.0; (2) Moberg (2005) -- © 2005, Macmillan Magazines Ltd.

Figure 3. Copyright note - Figure reproduced with permission from: Hegerl et al. (2007) -- © American Meteorological Society.

Figure 4. Copyright note - Figure reproduced with smoothing with permission from: (1) Rubino et al. (2019) – © CC By 4.0; (2) Ljungqvist (2010) - © The authors 2010, Geografiska Annaler: Series A © 2010 Swedish Society for Anthropology and Geography reprinted by permission of Informa UK Limited, trading as Taylor & Francis Group, www.tandfonline.com om behalf of Swedish Society for Anthropology and Geography.

Figure 5. Copyright note - Figure reproduced with smoothing with permission from: (1) Rubino et al. (2019) – © CC By 4.0; (2) Yang et al. (2002) -- © 2024. American Geophysical Union.

Figure 6. Copyright note - Figure reproduced with smoothing with permission from: (1) Rubino et al. (2019) – © CC By 4.0; (2) Ljungqvist (2010) - © The authors 2010, Geografiska Annaler: Series A © 2010 Swedish Society for Anthropology and Geography reprinted by permission of Informa UK Limited, trading as Taylor & Francis Group, www.tandfonline.com om behalf of

Swedish Society for Anthropology and Geography.

Figure 7. Copyright note - Figure reproduced with smoothing with permission from: (1) Rubino et al. (2019) – © CC By 4.0; (2) Yang et al. (2002) -- © 2024. American Geophysical Union.

Figure 8. Copyright note – Figure reproduced with smoothing with permission from: (1) MacFarling Meure et al. (2006) -- © 2024 American Geophysical Union; (2) Hegerl et al. (2007) -- © American Meteorological Society.

Figure 9. Copyright note – Figure reproduced with smoothing with permission from: (1) MacFarling Meure et al. (2006) -- © 2024 American Geophysical Union; (2) Yang et al. (2002) -- © 2024. American Geophysical Union.

Figure 10. Copyright note - Figure reproduced with permission from: (1) Rubino et al. (2019) – © CC By 4.0; (2) Hegerl et al. (2007) -- © American Meteorological Society.

Figure 11. Copyright note - Figure reproduced with smoothing with permission from: (1) Ahn et al. (2012) – © 2024. American Geophysical Union; (2) Frank et al. (2010) – © 2005, Macmillan Magazines Ltd.; (3) MacFarling Meure et al. (2006) -- © 2024 American Geophysical Union; (4) Rubino et al. (2019) -- © CC By 4.0; (5) Moberg et al. (2005) -- © 2005, Macmillan Magazines Ltd.; (6) Ljungqvist (2010) -- © The authors 2010, Geografiska Annaler: Series A © 2010 Swedish Society for Anthropology and Geography reprinted by permission of Informa UK Limited, trading as Taylor & Francis Group, www.tandfonline.com om behalf of Swedish Society for Anthropology and Geography; (7) Crowley (2000) -- © 2024 American Association for the Advancement of Science; (8); Hegerl et al. (2007) -- © American Meteorological Society ; (9) Jones et al. (1998) -- © 1998, Sage Publications; (10) Loehle and McCulloch (2008) -- © Multi-Science Publishing Co. Ltd.; (11) Juckes et al. (2007) -- © CC By 4.0; (12) Yang et al. (2002) -- © 2024. American Geophysical Union.

Figure 12. Copyright note - Figure reproduced with smoothing with permission from: (1) Ahn et al. (2012) – © 2024. American Geophysical Union; (2) Frank et al. (2010) – © 2005, Macmillan Magazines Ltd.; (3) MacFarling Meure et al. (2006) -- © 2024 American Geophysical Union; (4) Rubino et al. (2019) -- © CC By 4.0; (5) Moberg et al. (2005) -- © 2005, Macmillan Magazines Ltd.; (6) Ljungqvist (2010) -- © The authors 2010, Geografiska Annaler: Series A © 2010 Swedish Society for Anthropology and Geography reprinted by permission of Informa UK Limited, trading as Taylor & Francis Group, www.tandfonline.com om behalf of Swedish Society for Anthropology and Geography; (7) Crowley (2000) -- © 2024 American Association for the Advancement of Science; (8); Hegerl et al. (2007) -- © American Meteorological Society ; (9) Jones et al. (1998) -- © 1998, Sage Publications; (10) Loehle and McCulloch (2008) -- © Multi-Science Publishing Co. Ltd.; (11) Juckes et al. (2007) -- © CC By 4.0; (12) Yang et al. (2002) -- © 2024. American Geophysical Union.

Figure 13. Copyright note - Figure reproduced as original and with smoothing with permission from: (1) Ahn et al. (2012) – © 2024. American Geophysical Union; (2) Hegerl et al. (2007) -- © American Meteorological Society.

Figure 14. Copyright note - Figure reproduced as original and with smoothing with permission from: (1) Rubino et al. (2019) -- © CC By 4.0; (2) Hegerl et al. (2007) -- © American Meteorological Society.

Figure 15. Copyright note - Figure reproduced as original and with smoothing with permission from: (1) Rubino et al. (2019) -- © CC By 4.0; (2) Hegerl et al. (2007) -- © American Meteorological Society.